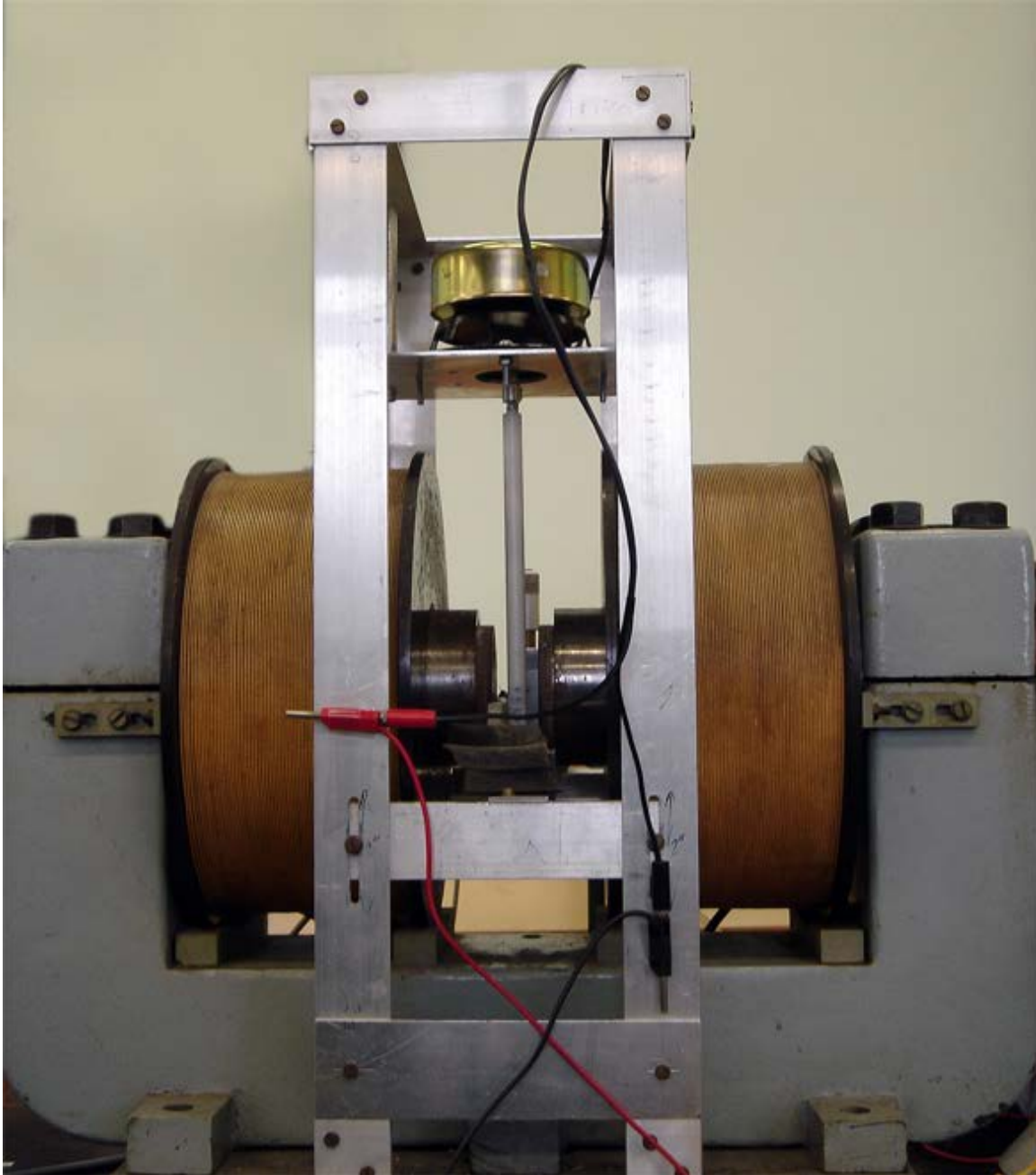


Vibrating Sample Magnetometer



By Stephen Mullens

Contents:

	Page Number
Abstract	4
Aims	4
Theory	
Ferromagnetism	5
Curie temperature	8
Crystal Structure	9
Hall Element	11
Method	
Apparatus	12
Calibrating the magnetic field	15
Finding the factors for magnetisation	19
Generation of varying magnetic fields	24
Interfacing with all the equipment	28
Progress indicators	30
Final Labview program	31
Results	
Magnetisation curves for different orientations	33
Consistency of the Experimental technique	36
Effect of changing the waiting time between readings	37
Altering Crystal Structures	39
Permanent magnets	42
Conclusion	43
References	44
Appendix	45

Abstract:

The effect of heating and physically damaging a cobalt wire is to deform its grain structure. This deformation converts a relatively uniform material to one with a significant number of defects; these defects interfere with the movement of the domain walls. With little deformation there is no evident hysteresis loop, a loop can be made visible by further deformation in the form of physical beating.

Aims:

The objective is to use a Vibrating Sample Magnetometer (VSM) to produce magnetisation curves for ferromagnetic materials.

Variables under consideration:

1. Orientation of the sample to the applied field
2. Physical changes to the samples structure – heating, oxidising

The data collection aspects of this project will be managed by a Labview (National Instruments) virtual instrument (vi). A modular part of a Labview virtual instrument will be referred to as a subvi.

Background Information:

The magnetic flux density \underline{B} in a ferromagnetic sample placed in a magnetic field of strength \underline{H} is:

$$\underline{B} = \mu_0(\underline{H} + \underline{M}) \quad \{1\}$$

\underline{B}	Magnetic Flux Density	Wbm^{-2}
μ_0	Permeability of Free Space	$\text{WbA}^{-1}\text{m}^{-1}$
\underline{H}	Magnetic Field Strength	Am^{-1}
\underline{M}	Magnetisation	Am^{-1}

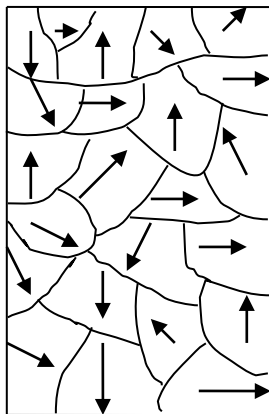
Ferromagnetism Explained:

The magnetisation in $\{1\}$ is the magnetic equivalent of polarisation in a dielectric. A Ferromagnet can be considered as a collection of magnetic domains; regions in the metal in which there is a small localised magnetic moment orientated in a random direction. These domains exist because of the characteristic microscopic ordering of electron spins in ferromagnetic materials.

When a field \underline{H} is applied in the region of the sample, the directions of the magnetic moments are forced to change in an attempt to align with the field.

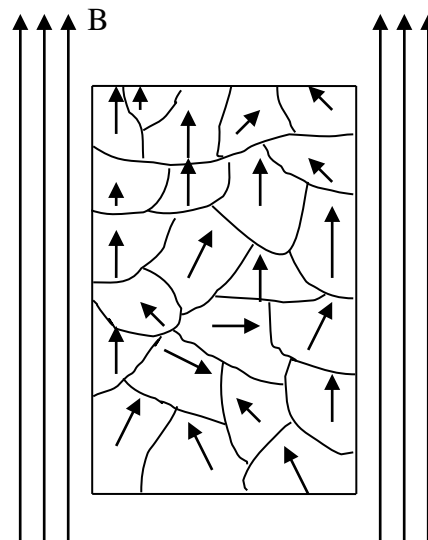
Figure 1 – Magnetisation Model

No External Field



$$\Sigma \underline{dm} = 0$$

External Field \underline{H} applied resulting in Field \underline{B}



$$\Sigma \underline{dm} > 0$$

As the duration or amplitude of the H field increase, the magnetic moments orientate to a greater degree which from $\{1\}$ will result in a larger B field. Work is done in orientating the domains magnetic moments in line with the external field and can be considered to be converted to potential energy; a loss of varying magnitude is converted to heat due to ‘frictional’ work between the domain boundaries.

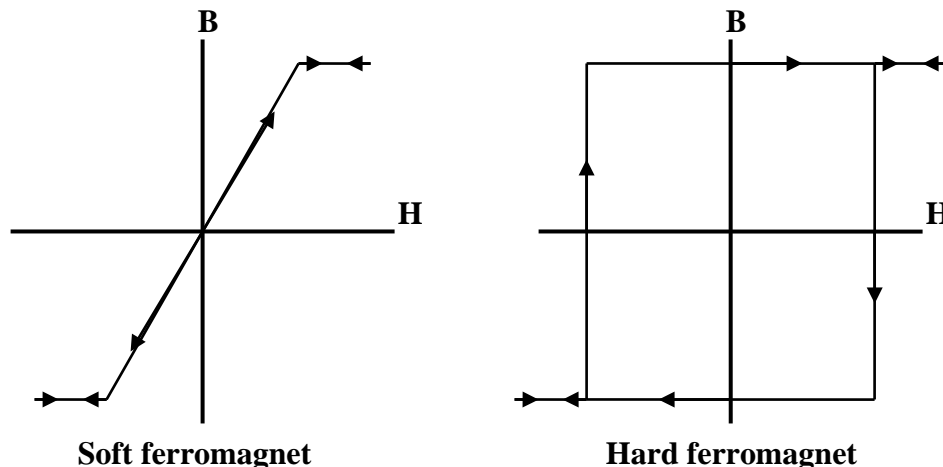
The point at which all the magnetic domains moments are orientated in the same direction, the saturation magnetisation has been reached with its value being the total magnetic moment of the sample; no increase in the external field applied to the sample will result in further internal magnetisation. If the field is removed after saturation magnetisation occurs, a remnant magnetisation is left. If the field direction were to be reversed then it would take a certain field strength H to fully cancel out the internal magnetisation of the ferromagnet, this field strength is known as the coercive field.

This model of ferromagnetism although very informative is technically wrong, from imaging of domains in single crystals it has been suggested that the application of an external field results in the shifting of domain boundaries in favour of the domains parallel to the applied field, the domains in line with the field grow in size at the expense of the surrounding boundaries.

Hard and Soft Ferromagnets:

The fundamental difference between ideally hard and soft ferromagnets is that the soft ferromagnet will have no remnant magnetisation whereas hard will have a high remnant magnetisation and coercivity.

Figure 2 – Ideal Hysteresis Loops

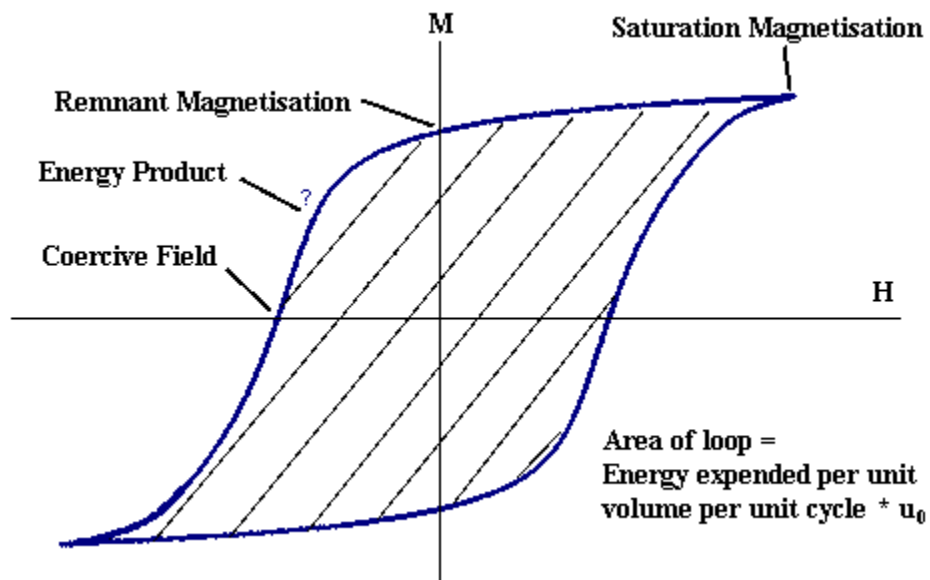


Hard magnetic materials are often called “permanent” magnets because once they have been magnetised their magnetic domains tend not to randomise. Additions of rare earth metals such as neodymium and cobalt to iron can transform iron into a very hard ferromagnet.

Soft magnetic materials have the ability to be magnetised, then magnetised the opposite direction with little energy loss in the Hysteresis loop. Typical applications for soft magnets are motors, generators and transformers where fast time varying field are required and heating of the material due to energy loss is not desirable. Silicon-iron and nickel-iron alloys are a common choice for the creation of soft ferromagnets.

The two graphs of ideal soft and hard ferromagnets (figure 2) are merely an idealisation of the perfect material, in practise materials are a combination of both characteristics. Some materials will produce a wide Hysteresis loop with a large area enclosed and others have a narrower loop with a corresponding smaller area, it is then possible to compare the two and say that the larger loop is produced by a harder material.

Figure 3 – Sample Hysteresis Loop



Hysteresis Parameters Explained:

Saturation Magnetisation is the limiting case where increasing the field strength around the ferromagnetic material will not yield an increased magnetisation. It is not practically possible to reach this point, although as the gradient of the Magnetisation vs Field strength curve approaches 0, then saturation magnetisation is close. Fitting an exponential equation to how the magnetisation increases with H and extrapolating it forward could lead to a more accurate indication of saturation magnetisation, but using this method the uncertainty in your result is limitless.

Remnant Magnetisation is a measure of how well a material will hold its magnetisation after an external field has been removed. The higher the value in relation to the external field, the harder the magnet.

Coercive Field is the external field which needs to be applied to counteract the remnant magnetisation in the sample and reduce the magnetisation to zero.

Curie Temperature: ref [3], [4]

The Curie temperature of a ferromagnetic material is the point where thermal fluctuations randomly realign all the domains, turning the ferromagnet into a paramagnet, reducing the net magnetisation to approximately zero (figure 4). Paramagnets do have some net magnetisation but it is many orders of magnitude weaker than ferromagnetism. This realignment also occurs below the critical curie point but becomes increasingly less significant as the temperature is lowered.

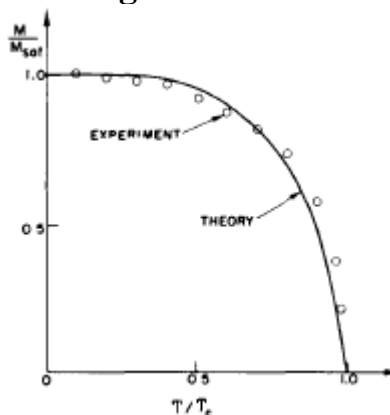
In this experiment it will be essential to choose ferromagnetic materials with Curie temperatures well above room temperature of $\sim 300\text{K}$.

Suitable materials:

- Iron (Fe) – 1043K – bcc structure
- Cobalt (Co) – 1388K – hexagonal structure
- Nickel (Ni) – 627K – fcc structure

Materials such as Gadolinium and Dysprosium are not suitable because their Curie temperatures are 292 and 88K respectively. If a sample of Gadolinium were to be cooled with liquid nitrogen then it would be more than possible to detect ferromagnetism, however the practical difficulties in maintaining a low temperature would be significant.

Figure 4 – Ferromagnetism and curie temp (ref 3)



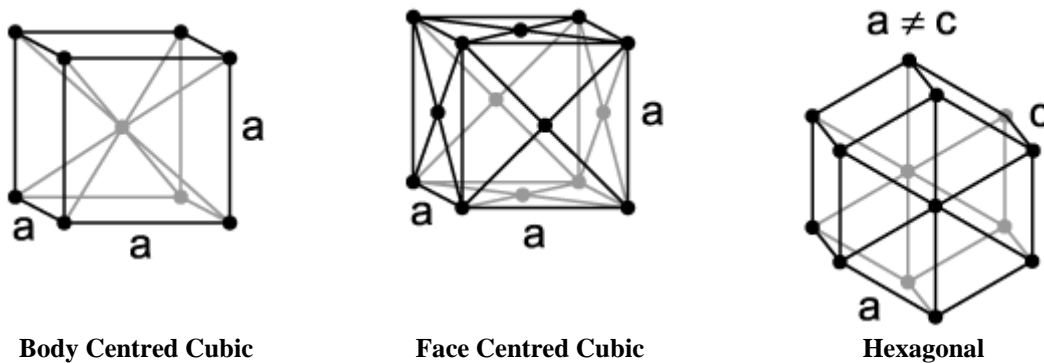
Crystal Structure: ref [1]

Listed with the possible samples are their respective crystal structures, these structures are the fundamental building blocks in which atoms pack together. When a liquid metal is cooled into a solid, the atoms align into their lattices as energy is lost, typically this results in a polycrystalline solid containing multiple crystals. Multiple crystals are formed because many crystals form simultaneously at different locations and merge together at their boundaries, often referred to as grain boundaries, in this experiment all materials will be polycrystalline because of the financial cost of acquiring large single crystals.

There are two extreme cases of metallic crystallisation, the first being where a sample is made up of a single perfect crystal and the second where no crystals are allowed to form. Both of these situations are related to the speed at which the liquid metal is cooled. If a liquid is cooled very slowly so that only one crystal can form then a giant crystal lattice will be formed.

If a liquid is cooled extremely quickly then the atoms do not have time to travel to a lattice site before their motion is restricted by the low temperature, this results in no crystals and this state is referred to as an amorphous material.

Figure 5 – Typical Crystal Structures



Defects in the crystal structure:

There are many types of possible defects in the crystal structures of ferromagnetic materials, any defect can affect the manner in which a material magnetises. Common types of defect are listed below.

Vacancies are sites which are usually occupied by an atom but instead there is an empty space, the stability of the crystal lattice will prevent a collapse into the void.

Interstitial are atoms which occupy a space in a crystal lattice which is not normally occupied by an atom, hydrogen is small which allows it to exist in crystal structures. The addition of these additional atoms can result in a local distortion of the structure.

Impurities exist in all materials because of the impossible task of removing all unwanted atoms, impurities can often be incorporated into a regular part of the crystal structure.

The addition of large quantities of nickel, chromium and nitrogen to iron can alter the crystal structure to a face centred cubic; the resulting metal is referred to as Steel.

Dislocations occur when a plane of atoms inside the crystal terminates early resulting in the surrounding planes bending in an attempt to fill this gap, this is common in the structure of graphite which is a layered material. This effect can be compared to inserting half a piece of paper into a large stack and the other pages bend to compensate.

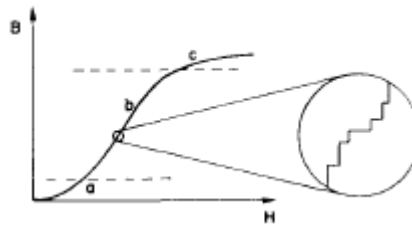
Grain boundaries are where two crystals boundaries meet resulting in the direction of their lattices abruptly changing.

Stacking Faults can occur when crystal layers stack in a strange order. For example face centred cubic structures differ from hexagonal close packed structures only by the order the layers stack together. Typically one structure is more likely to form than the other. Depending on the material, extreme conditions and different production techniques can result in the varying of the structure from the standard.

The Barkhausen Effect – ref [2]

When a ferromagnetic material is placed in a magnetic field, impurities, dislocations, grain boundaries or imperfections in a crystal structure can result in the domain wall getting stuck when trying to move. If a domain wall is stuck and the field strength around the material is slowly increased, there will be a specific point where the domain wall will suddenly shift, this is analogous to how earthquakes occur. The result of this is a jerky magnetisation curve where the magnetisation of a sample does not vary smoothly with external field strength, this effect is typically only noticeable when approaching saturation magnetisation.

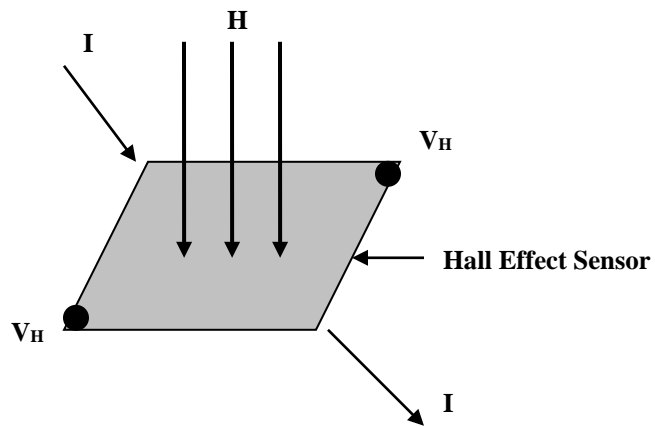
Figure 6 – Jerky magnetisation (ref 2)



The Hall Element: ref [5]

The Hall effect sensor is a semiconductor device with current flowing through it. When a magnetic field penetrates the sensor at 90° to its surface, a voltage is induced perpendicular to the current path. This voltage varies approximately linearly with field strength.

Figure 7 - The Hall Effect Sensor



In this experiment the Hall sensor is parallel with the field from the large magnet so the field should have minimal effect on the Hall voltage. When the loudspeaker oscillates the sample rod, and in turn the sample; the ferromagnetic sample will magnetise and a component of its field will enter the sensor resulting in a Hall voltage.

$$V_H = \frac{M\gamma_c d \sin(\omega t)}{2} \quad \{2\}$$

M	Magnetisation detected	Am^{-1}
γ	Hall Sensitivity	$\text{VI}^{-1}\text{A}^{-1}\text{m}$
I_c	Current through Hall Element	I
d	Amplitude of oscillation	m
ω	Angular frequency of sample oscillation	s^{-1}

$$\gamma = \frac{V_H}{IH} \quad \{3\}$$

V_H	Voltage from the Hall sensor	V
I	Current through the Hall sensor	I
H	Magnetic field perpendicular to Hall surface	Am^{-1}

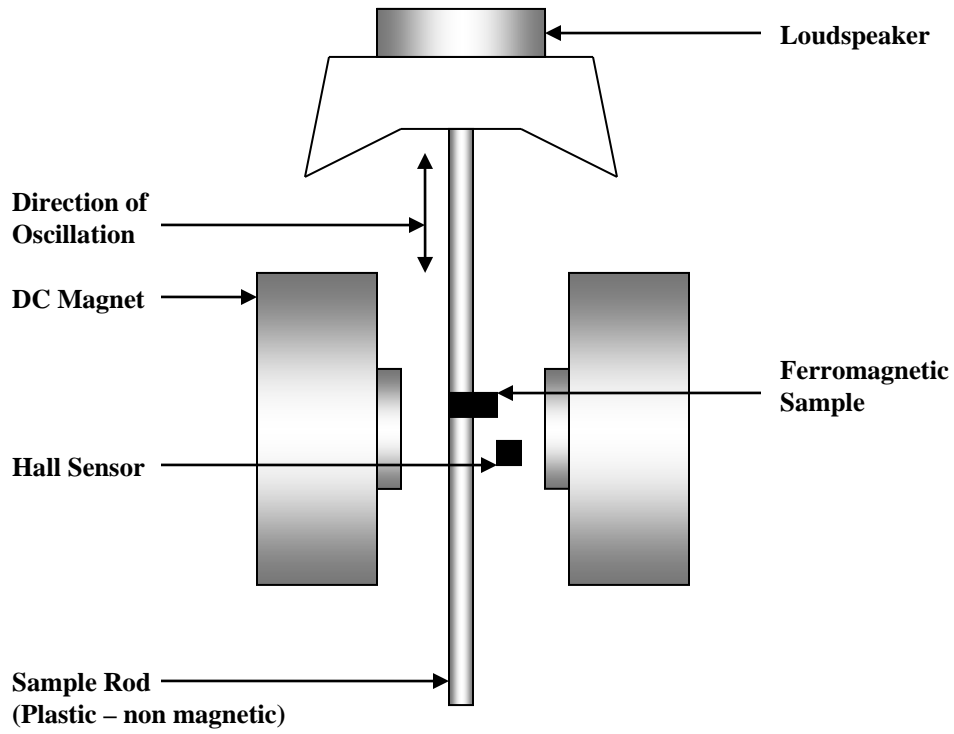
Rearranging to find the magnetisation and remove the oscillating term which is removed by the lock-in amplifier.

$$M = \frac{2V_H}{dI_c\gamma} \quad \{4\}$$

The magnetisation detected is proportional to the magnetisation in the sample where the constant of proportionality is related to the mean distance between the hall sensor and the nearest face of the ferromagnetic sample. When comparing data from different samples it will be important to maintain the same distances such that magnitudes of magnetisation can be compared.

Apparatus:

Figure 8 - The Vibrating Sample Magnetometer



Orientation of Magnets and Sensors

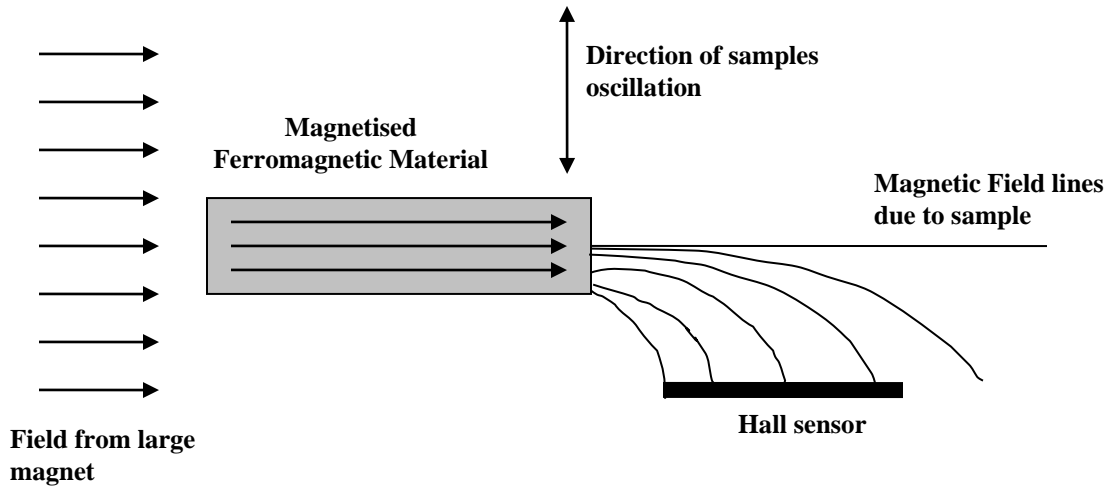
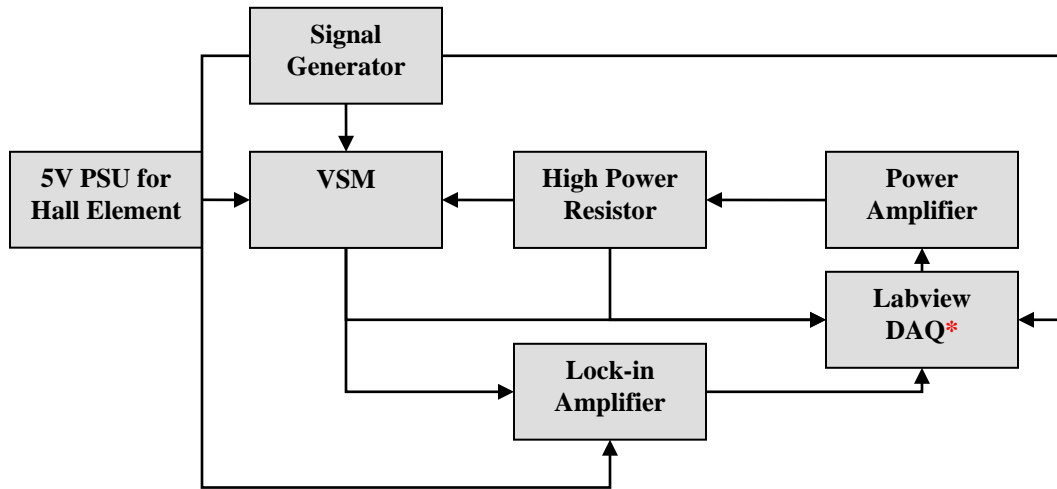


Figure 9 - The Setup



* DAQ = Data acquisition

Discussion of the Apparatus:

The signal generator drives a loudspeaker which oscillates the sample in the magnetic field. The frequency driving the oscillation is fed into Labview and recorded. Another output from the frequency generator is sent to the lock-in amplifier for use as a reference signal

The 5V power supply is used to power the Hall element. The current is also maintained at constant level.

The output from the VSM is an induced voltage from the Hall element which is connected to the lock-in amplifier and compared against the reference signal. Another copy of the Hall element voltage is sent to Labview for further analysis and graphed to ensure that the system is working.

The output from the lock-in amplifier is a DC voltage representing the in-phase voltage from the Hall element. When this voltage is multiplied by the sensitivity setting of the lock-in amplifier, the RMS hall voltage is obtained.

The High Power Resistor

The power amplifier receives an input voltage from the Labview DAQ card (-10 to +10V) which it then scales up to power the large magnets. There is a high power resistor which connects to the negative terminal of the power amplifier and is in series with the magnets coils. The important characteristics of this resistor are that it has a low

impedance compared to the magnets coils and is able to dissipate heat faster than it can build up, with the goal to maintain a constant temperature.

The voltage across the power resistor will be proportional to the current flowing through the magnets coils at all times presuming that the resistor is operating and a constant temperature. The appreciation of this statement will solve the problem that arises when the magnet changes temperature. This point is best illustrated by consideration of how the field produced by the magnet will vary if the Labview driving voltage is constant.

As power flows through the coils energy is lost as I^2R in the form of heat, the magnet heats up which increases the resistance of the coils, which in turn lowers the current flowing because $V = IR$ (The power amplifier delivers a constant voltage). The field strength between the coils is a function of the current flowing and not the voltage, the current through the power resistor is the same as the coils and because the resistance of the power resistor is approximately constant, the voltage across it is proportional to the current flowing. The constant of proportionality and the resistance are of no interest, it will be shown later how an equation can be produced to convert resistor voltage to field strength. This conversion equation is not expected to be linear because of hysteresis in the large iron cores from which the electromagnet is built.

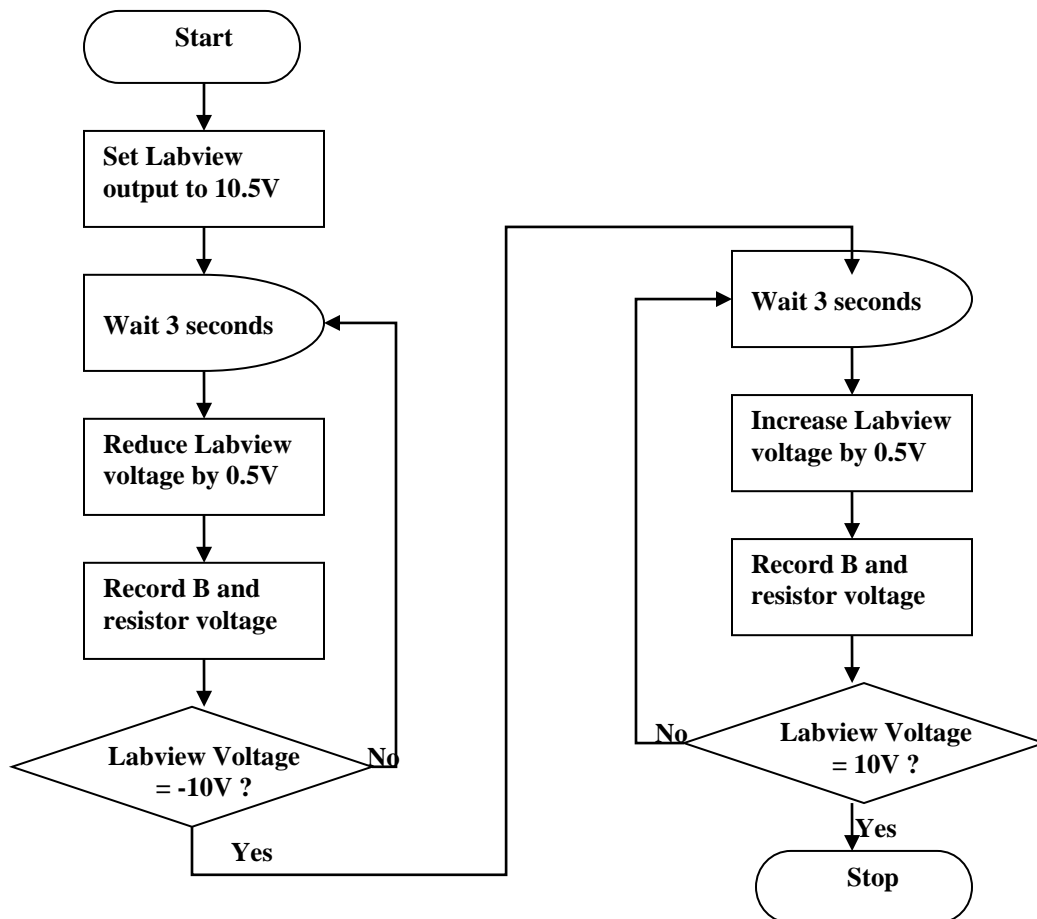
The field strength surrounding the sample varies from approximately -800mT to 800mT with the given voltage input range. The maximum output voltage from the power amplifier is of the order of 60V, as such all contacts will be electrically insulated to prevent accidental electrical shock.

Calibrating the large magnetic field:

The field is generated by sending a DC voltage to a power amplifier which amplifies the signal and uses it to powers a large set of coils. The voltage range which is to be sent by Labview is $\pm 10V$. The voltage range should be looped through from +10V to -10V and back to pick up any hysteresis in the large coils.

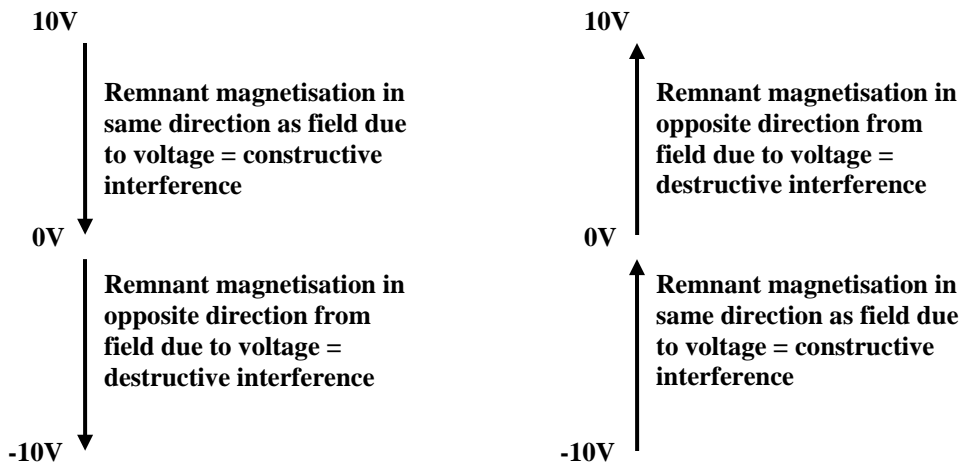
The field strength inside the magnet can be measured by placing a calibrated Hall probe in the space between the two poles of the magnet then reading off the field strength from its indicator. The oscillating part of the system should be removed when carrying out these readings to ensure no interference effects, although the magnetisation in the sample is expected to be negligible compared to the field created by the magnets. Time should be allowed for the power amplifier and magnet to adjust and settle down before readings from the calibrated Hall sensor are taken. It is important that for all readings taken, a time delay is used to ensure that the system has had time to adjust to the new voltages. A step length of 0.5V should result in a good range number of points.

Figure 10 - Process to take readings for calibration of magnet



The voltage across the resistor should be plotted against the field strength from the calibrated hall sensor, this should yield a loop, with one side of the loop representing the positive to negative Labview voltage and the other from the negative to positive voltages. This effect is due the remnant magnetisation of the large iron cores in the magnet interfering constructively and destructively depending on the position of the loop. A simple method to show that hysteresis effects exist in the large magnet is to set the magnet to full power then turn the power off and you will observe a residual field, this is due to a remnant magnetisation.

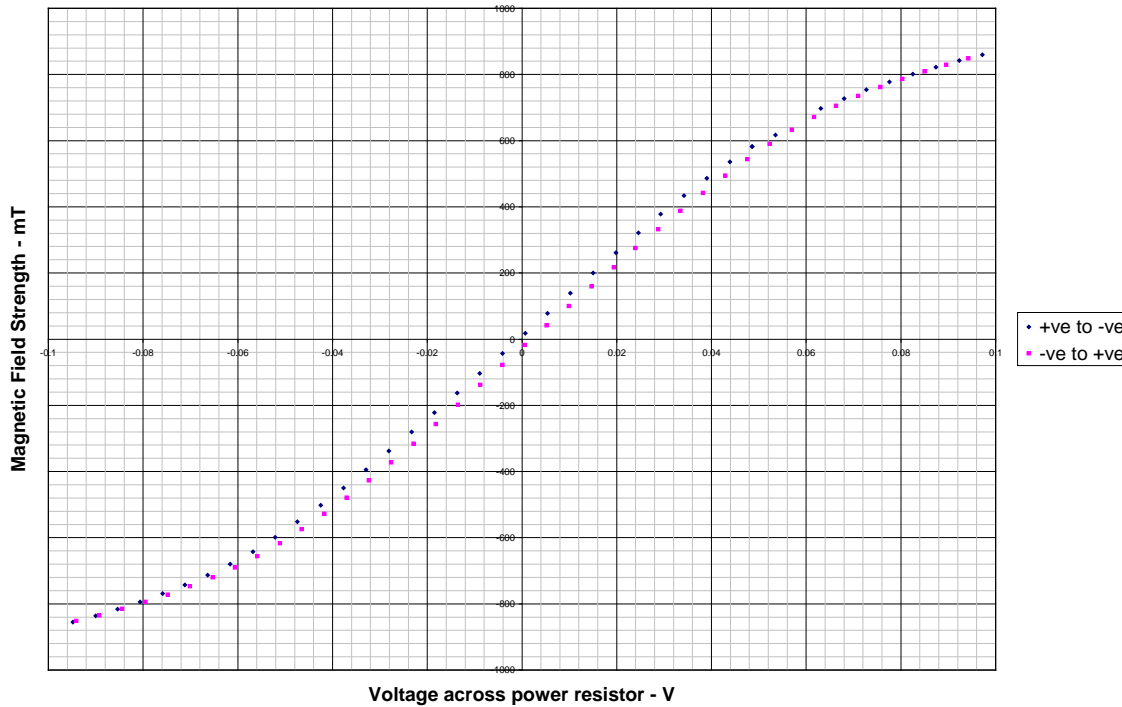
Figure 11 - Understanding Hysteresis in the Large Magnet



Calibrations for each side of the loop can be made by using a curve fitting program to fit equations to each side. The equations should be such that $y = f(x)$ where y is the field strength between the magnet poles and x is the resistor voltage. The type of equation to fit to the data is not of great significance so long that it is a good fit to the data points within the whole range, divergence after this is not significant because voltages in this range will not be used. The equation for each side of the fit can be built into Labview calibration subvi to convert from the resistor voltage to the H field strength.

A program to interface with the hardware to collect data for this calibration can be found in the appendix. It gives the user the ability to send user defined voltages to the power amplifier.

Figure 12 - Calibration graph for the magnetic field



+ve to -ve voltages

$$\text{Magnetic Field Strength (mT)} = 12.66 + 12707V - 3035V^2 - 42491V^3 + 182101V^4$$

-ve to +ve voltages

$$\text{Magnetic Field Strength (mT)} = -28.60 + 12761V + 4323V^2 - 435383V^3 - 136540V^4$$

From equation {1}, the conversion from a B field with mT to an H field with Am^{-1} is:

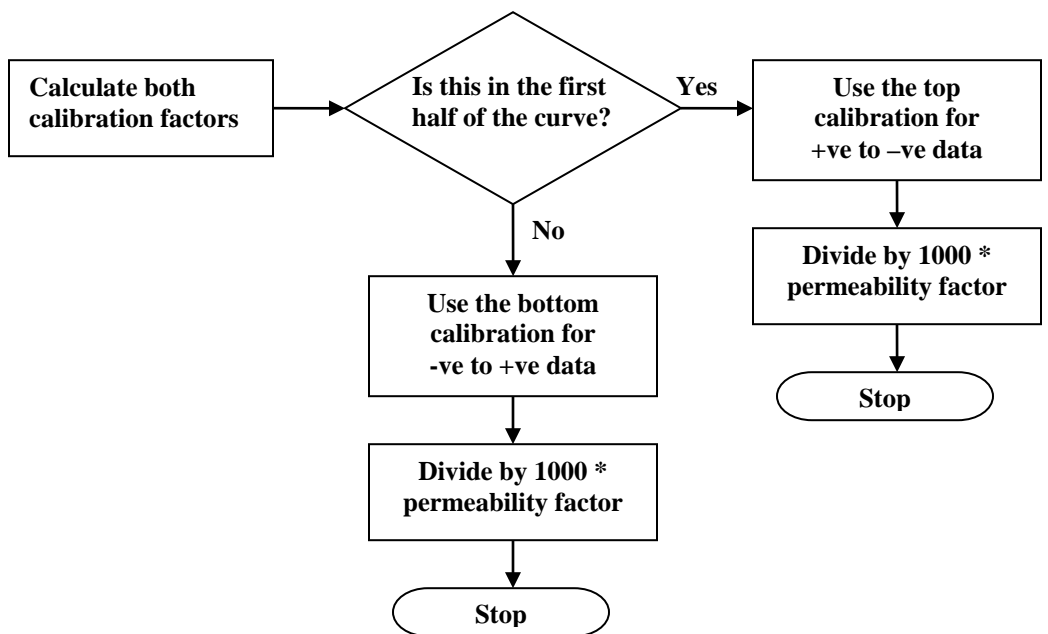
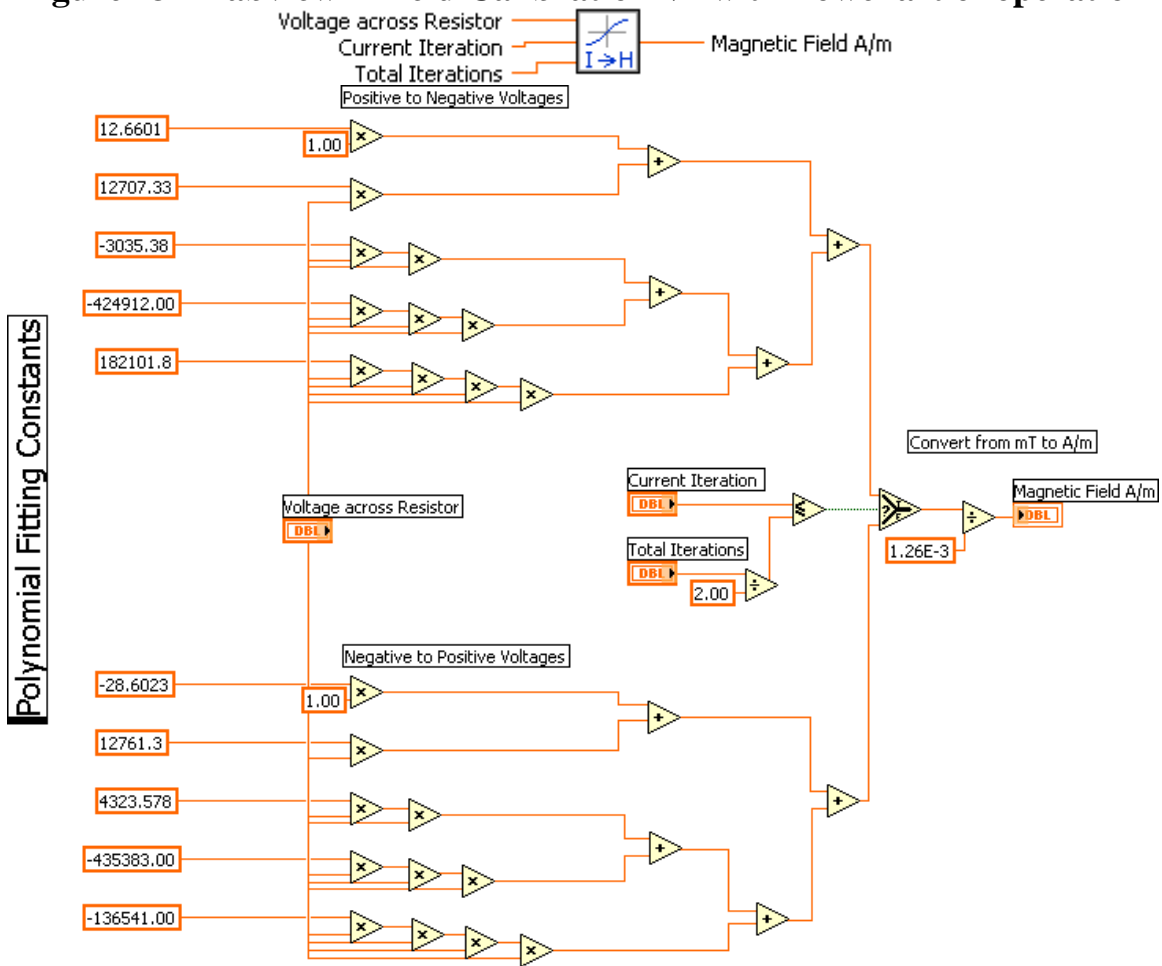
$$\text{Am}^{-1} = \frac{mT}{1000\mu_0} = \frac{mT}{1.257 * 10^{-3}} \quad \{5\}$$

The initial calibration used mT units because that is what the calibrated Hall probe measured in, this is perfectly acceptable but conversion to Am^{-1} units is desired.

Figure 13 is a calibration which will convert both sides of the loop to their true field value, the flow chart summaries how the operations are processed. The assumption this VI makes when deciding which calibration to use is that there are an equal number of sample of data taken for each side of the loop. In the same time is spent travelling from +ve to -ve voltages and from -ve to +ve voltages.

The efficiency of this virtual instrument could be improved by first deciding which calibration to use by looking at iteration numbers, then using a True/False case structure to choose which calculation to do. This would make the program run almost twice as fast but because processing speed for something this simple is not an issue, a more visually descriptive method has been used.

Figure 13 - Labview H field Calibration VI with flowchart of operation



Finding the Factors for Magnetisation:

From equation {4} the factors which need to be established to find the magnetisation at the Hall sensor have been isolated and methods to work them out have been explained.

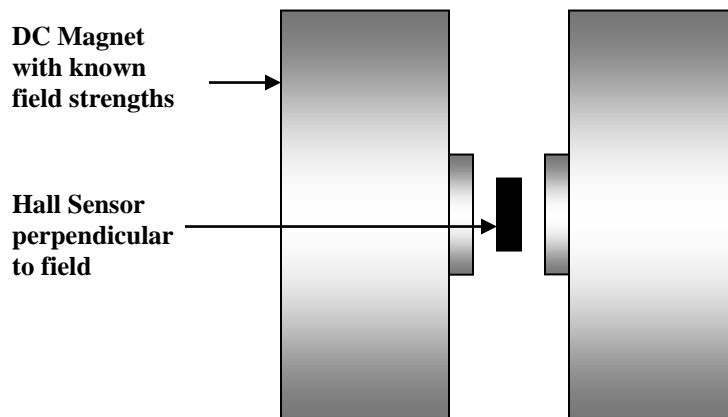
$$\underline{I_c \gamma}$$

This term is the sensitivity of the Hall element times the current passing through it. Measuring the rate of change of the Hall voltage with respect to known field strengths will yield a result. Such that:

$$\frac{dV_H}{dH} = \gamma I_c \quad \{6\}$$

The field from the large magnets is varied and the voltage from the Hall element recorded. Low field strengths should be used such that the Hall element just saturates on both the positive and negative fields and many data points lie between. The gradient of the linear transition should be measured and is equal to $I_c \gamma$.

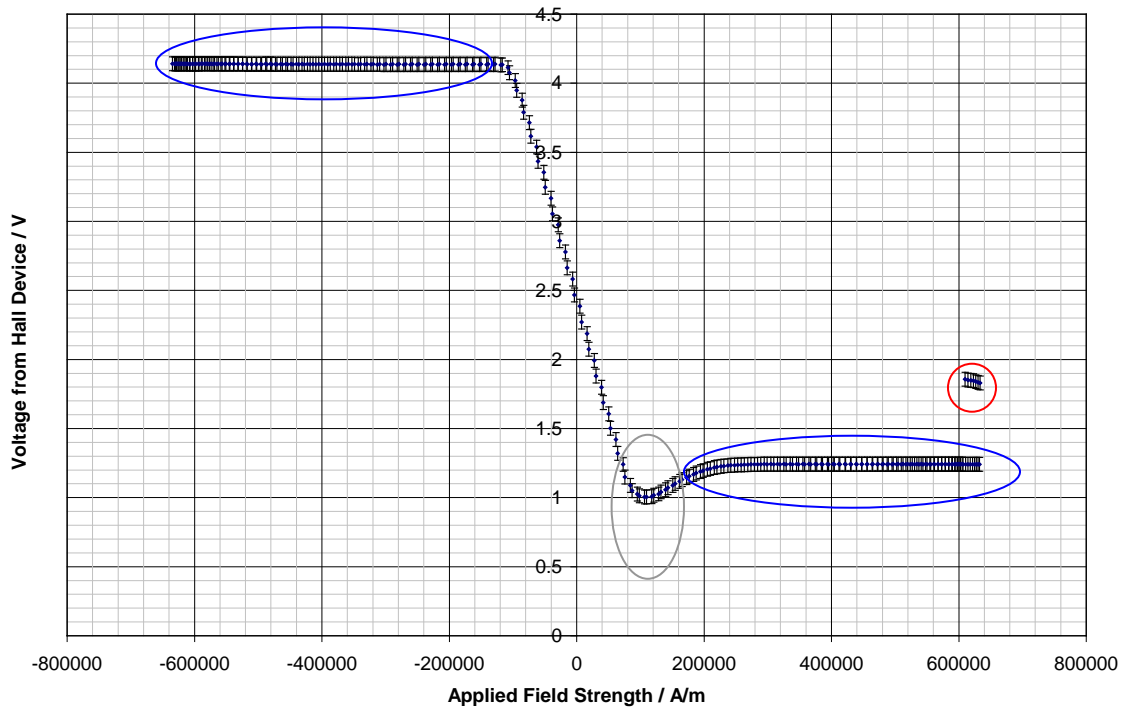
Figure 14 - Varying the field to find Gamma I



The setup for these readings requires that the Hall sensor is exposed to the entire magnetic field produced by the large magnets and that the vibrating part of the system removed. It is also important to make sure that the current through the hall element is constant throughout the experiment; this can be achieved by placing an ammeter in series with it. As with calibrating the large magnetic field, a time delay should be included between taking readings and altering the magnet power to give the system time to adjust.

Figure 15 shows how the hall element responded to varying fields perpendicular to its surface. To find the $I_c \gamma$ factor, the section of interest is the straight line which intersects the Hall voltage axis; however there are some anomalies which should be addressed for completeness.

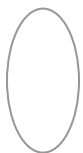
Figure 15 - Response of the Hall sensor with varying fields



These anomalous points are a result the large magnetic field causing part of the apparatus to collapse into between the centre of the magnet. The part in question was responsible for supporting the bar to which the hall sensor was mounted, this resulting in the Hall sensor partially moving out of the field. This is a clear illustration of the dangers of having ferromagnetic materials near such a strong magnet.



These points are where the Hall sensor output is saturating, an increase of field strength has a negligible effect on the Hall voltage. Increasing the voltage which drives Hall element may allow for larger field strengths to be measured, but without having a copy of the datasheet it is uncertain whether larger voltages would damage it.



The cause of this rise in Hall voltage is unknown. It could be an artefact of the response of this particular sensor, but never the less, it is not relevant to this experiment.

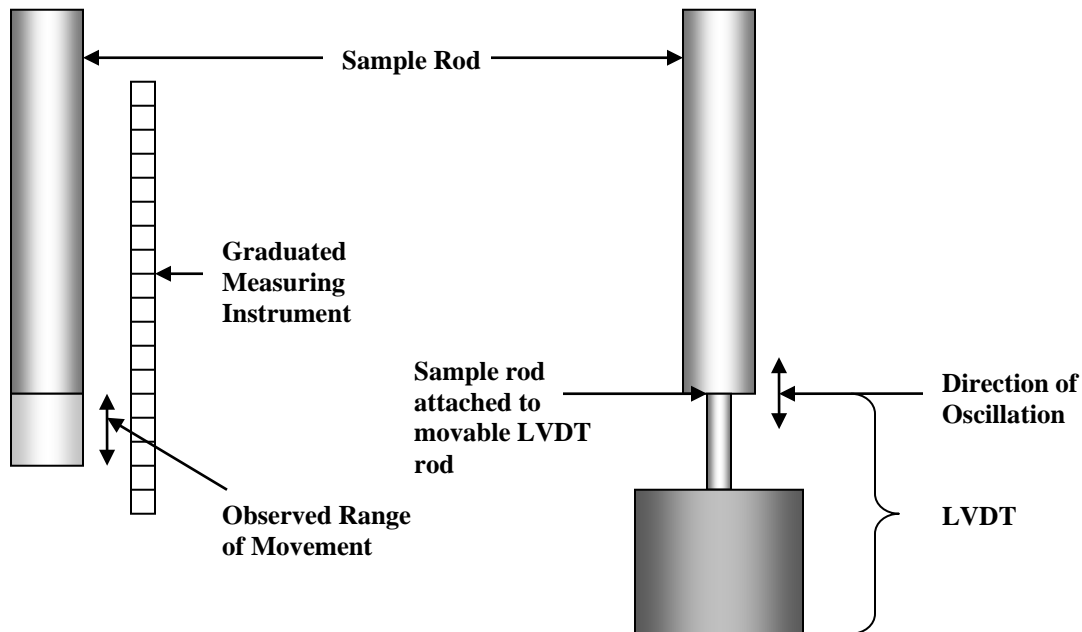
From the line which intersects the Hall voltage axis:

$$|\gamma I_c| = 1.71 \pm 0.03 * 10^{-5} VA^{-1}m$$

d

This factor is simply the amplitude of the oscillation of the sample. There are many possible methods to measure this quantity, the simplest being to hold a finely graduated ruler against an end of the sample rod and estimating the distance. A more sophisticated method would be to attach a position sensor to the bottom of the sample rod and use Labview to read in the data from it, a suitable sensor would be a Linear Variable Differential Transformer (LVDT).

Figure 16 - Simple techniques for measurement of



Due to budget limitations and because the magnetisation equation is only proportional to the actual magnetisation, it has been decided to use a finely graduated metal ruler to measure the amplitude of oscillation. This value will be re-measured for each set of readings taken because the system is very sensitive to changes, a slight change can alter the friction on the sample rod and drastically affect the amplitude of oscillation. The large magnet should ideally be switched off before measurement of the distance to prevent risk of electrocution and the ruler being moved the large magnetic field. It has been noticed that on activation of the magnet, the amplitude of oscillation changes, this is likely due to a small fraction of the magnets field interfering with that of the speaker, the magnitude of this effect is likely to vary as the field strength between the poles changes but is very difficult to quantise. For the purpose of this experiment the amplitude of oscillation will be assumed to be constant for each run of the system.

A typical value for d is 2mm. This value can be adjusted by changing the driving voltage to the speaker via the signal generator, or altering the frequency. Lower frequencies tend to result in larger oscillations due to the energy which needs to be expended by the loudspeaker to move the heavy sample rod. There are some resonances in the system for particular frequencies which cause the oscillations to become large as

well. Suitable frequencies to drive the system which result in good oscillations vary from 10 to 30 Hz.

A further consideration in determining the amplitude of oscillation is that the oscillation will not be sinusoidal; this is a result of the sample rod's mass. When a weight is attached to the speaker cone it is displaced from its central position and hence the speaker will move out of its linear range more quickly for a downward displacement than an upward one. The amplitude of the oscillation will have to be considered to be half the maximum movement by the sample.

One possible method to make the oscillation more sinusoidal is by exerting a force to balance out the mass of the sample rod. A spring could be attached to the bottom of the sample rod and a surface below it, such that at all points during the oscillation the spring is compressed and hence exerting a force on the sample rod; the magnitude of this force is unlikely to be constant, but it should still improve the oscillation.

V_H

This factor is $\sqrt{2}$ multiplied by the DC output from the lock-in amplifier multiplied by the lock-in Amplifiers sensitivity. It is essentially the range through which the voltage from the Hall sensor changes.

Distance between Hall sensor and sample

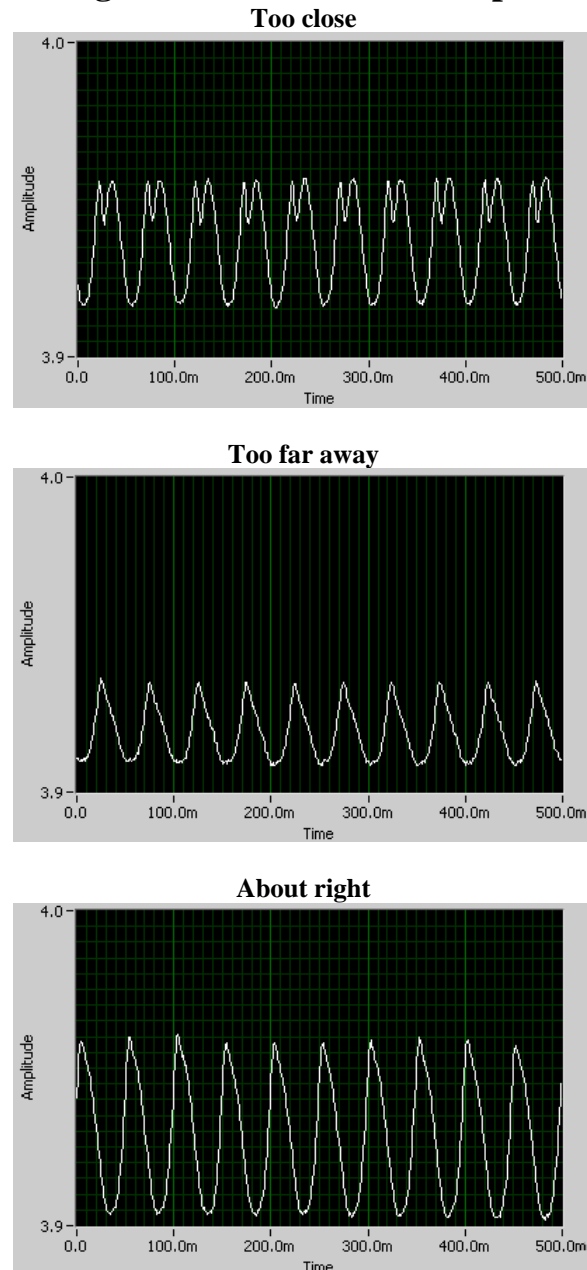
The magnetisation parameter defined earlier is only proportional to the magnetisation where the constant of proportionality is based upon the distance between sensor and sample and the shape and size of the sample. If all of these can be maintained through the experiment then comparative magnetisation values can be found, however this is very difficult. When swapping samples to be measured in the VSM, it is necessary to take apart some of the apparatus before doing so, then reassembling after. The most important variable will be the distance from the Hall sensor to the ferromagnetic sample, this distance is very small and at its closest point will be of the order of 1mm from the sensor, measuring a distance as small as this accurately would be very complicated because of very restrictive access to the moving parts of the system.

The method to be used to ensure that the sample is about the same distance from the sensor for each experiment is to oscillate the sample in a field and move the sensor using a vernier scale until the shape of the hall sensor output looks a certain repeatable way.

Figure 17 shows three possible situations. When the hall sensor is too close to the sample there is risk of collision and rapid changes of air pressure, these two problems are likely the cause of the top peak reversing in on itself.

The graph which is too far away has very small amplitude and the shape of top and bottom turning points are very different. When the hall sensor is moved slightly closer to the sample then a graph similar to the final graph can be produced; the hall output from this is far from being a true sine wave, but it is acceptable. If this approximate shape can be produced (amplitude may vary between different materials) again and again, then it can be assumed that the small distances between sensor and sample are approximately constant.

Figure 17 – Hall sensor output



Generation of Labview Output Voltages:

It is essential to create a means by which to automate the data collection process. An important part of this is to make a Labview program which can send out voltages to the power amplifier to alter the field strength in a desired manner.

Requirements:

- Loop through a voltage range from +x to -x to +x volts
- Have the field change for y number of points between the loop range
- Be able to alter how the points are distributed over the range of voltages, i.e. be able to put more points in the voltage ranges where most variation in magnetism occurs.

One way to achieve these requirements is to make a distribution of voltages which varies linearly over the voltage range, then a separate scaling factor can be applied to the voltage range to concentrate the points in the desired area.

Figure 18 - Creation of a linearly changing voltage

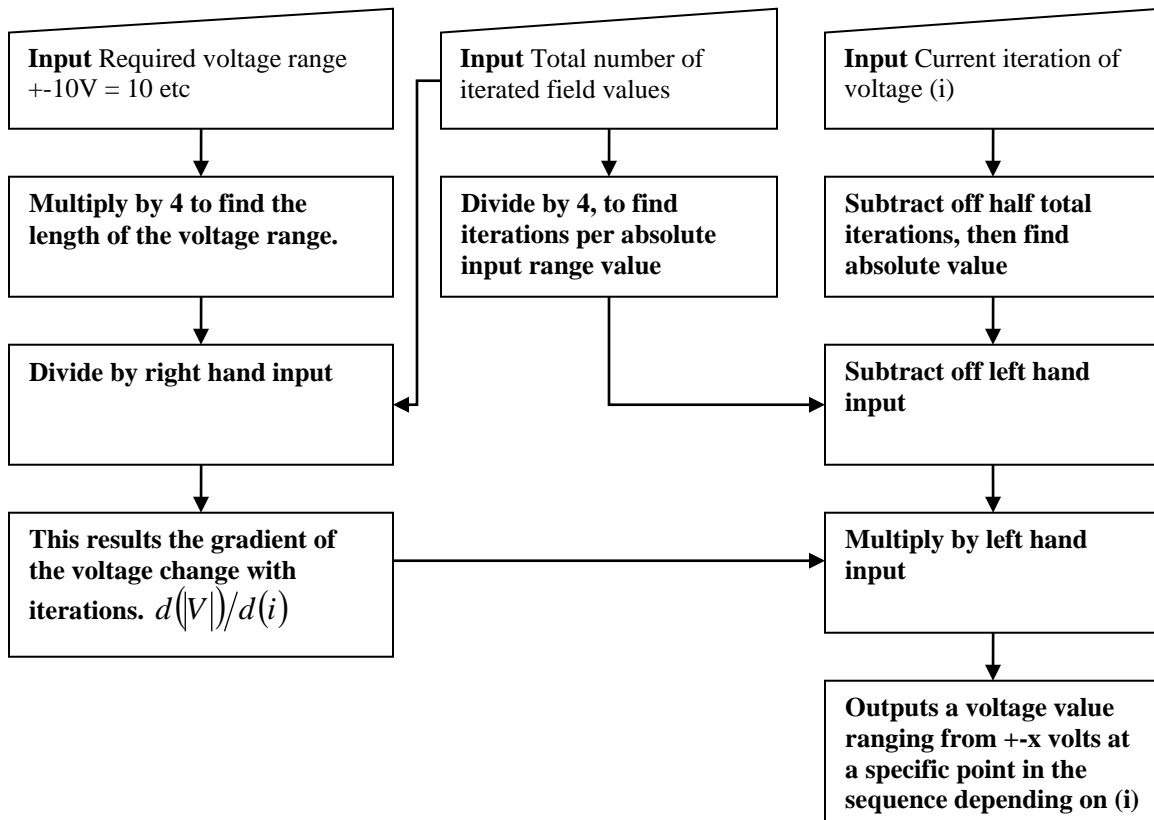


Figure 18 yields an output voltage which changes linearly in magnitude with the current iteration value. E.g. if the input range was 2 volts and a total of 9 iterations, then with 'i' ranging from 1 to 9, voltages would output as 2,1,0,-1,-2,-1,0,1,2. If the number of iterations is not 1 plus a multiple of 4 then the program will slightly shorten the range, but

this is not important because the area of interest in hysteresis loops is often at the low field strengths.

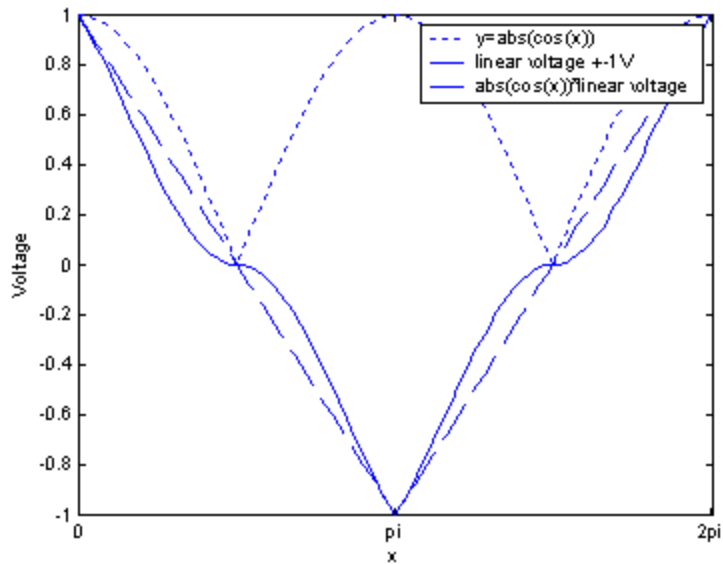
The next stage is to map distributions onto this linearly changing voltage range so that finer changes in the field strength are made at low field values. The two possible methods to be discussed are a multiplication of a cosine or a squared distribution onto the linear range.

Cosine Distribution:

Figure 19 shows the effect of mapping a cosine curve tactically onto the linear voltages created by Labview. By multiplying the absolute value of the cosine curve with the linear voltages it causes the resultant curve to spend longer at lower voltages, hence produce more data points about 0 field strength.

The Matlab code used to create this graph can be found in the appendix.

Figure 19 – Cosine distribution mapping



The precise mathematical relationship for these distributions to map together in this way is:

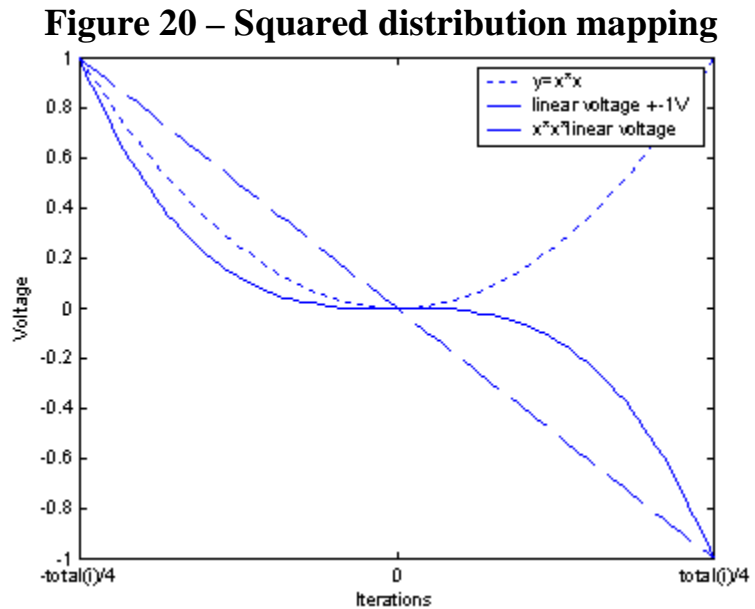
$$V_{new} = \left| \cos\left(\frac{2\pi i}{total(i)}\right) \right| \cdot V_{old} \quad \{7\}$$

i	Iteration number
V_{old}	Voltage from linear distribution
V_{new}	New voltage

This ensures that the start middle and end values of the cosine function occur at the correct times in relation to linear voltage generation.

Squared Distribution:

The squared distribution is more centrally focussed than the cosine. It works by splitting the distribution into 2 pieces. The first piece travels from x to $-x$ volts and the second $-x$ to x volts. It then multiplies a suitable positioned squared function centred at 0 volts over the old linear voltage. Figure 20 only shows the first half of the linear voltage.



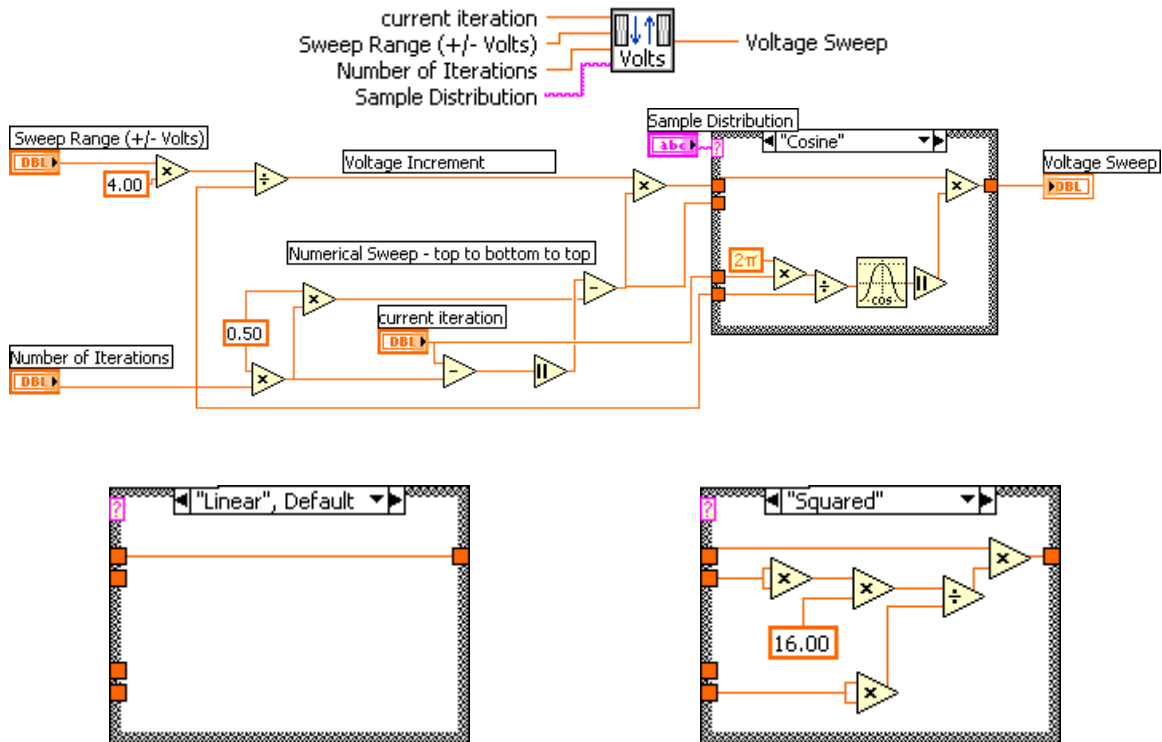
The x axis limits show that at \pm total iterations / 4, the square distribution must be equal to one. For this to be the case the following mathematical condition must be met.

$$y = \frac{16}{I^2} x$$

- {8}**
- y Multiplication factor for linear to V_{new}
 - x A measure of the position of the current iteration relative to the current half of the distribution
 - I Total number of iterations

Both of these distributions and the linear distribution have been built into a Labview virtual instrument, see figure 21. This subvi takes information in from another program and outputs a single voltage value for the point in the loop where it thinks it is.

Figure 21 - Labview Program to create voltage distributions



This Labview virtual instrument takes a string input to decide which distribution to use, the required input strings are "Squared", "Linear" and "Cosine". By default if no distribution is specified it will just output voltages corresponding to the linear distribution.

Interfacing with the apparatus

Figure 22 - Interfacing with the real world

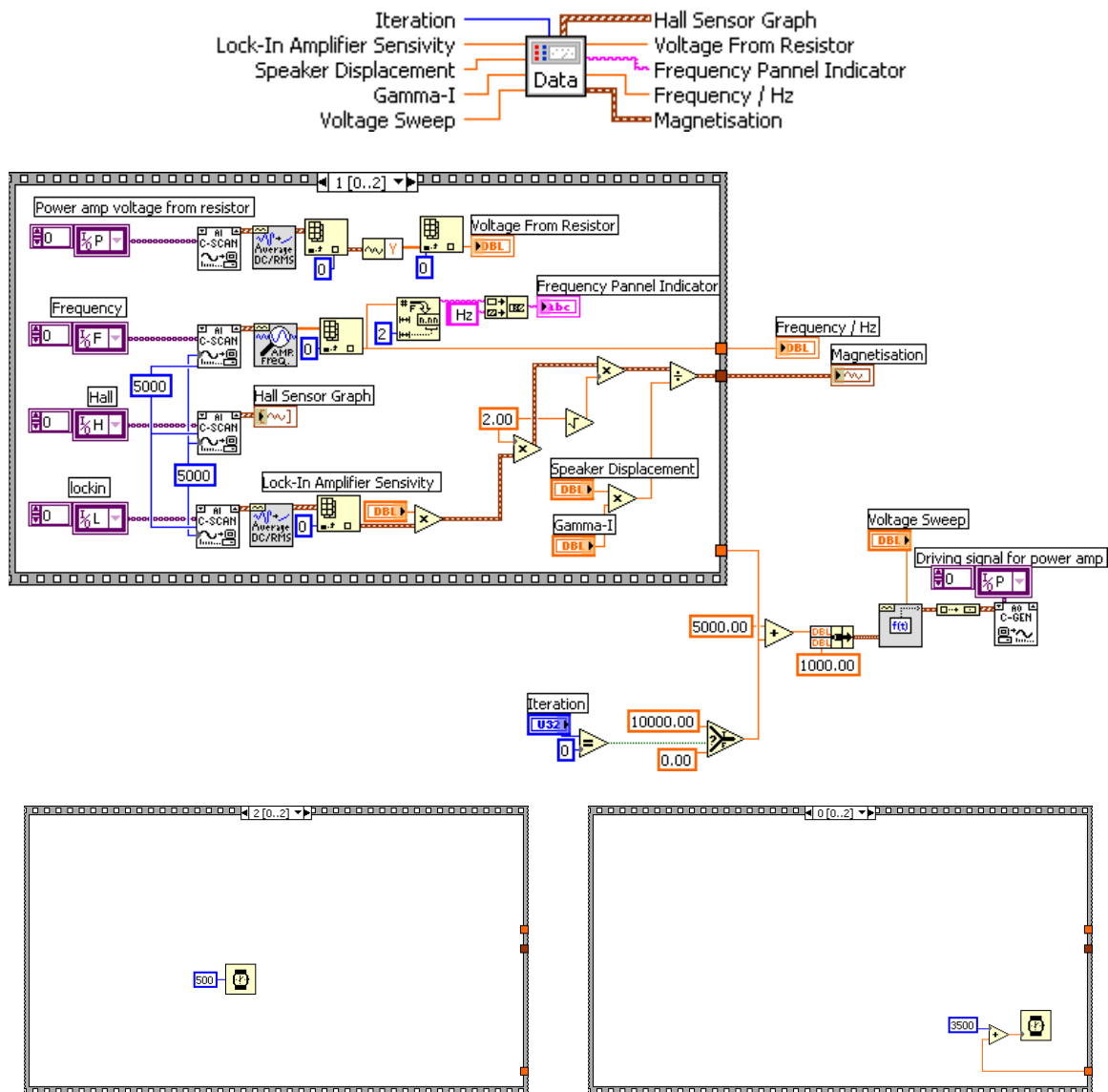


Figure 22 shows how the data input and output is managed in Labview. This program is designed to be looped and at the start of each loop a dc offset voltage is sent via an analogue output to the power amplifier, because of the nature of how Labview outputs, the output level is maintained even after the program stops running, until a different signal is sent.

During the time the signal is being sent, the first stage of the sequence waits for 3.5seconds to allow the amplifier time to adjust its output and the magnetic field settle down. After the waiting time has elapsed, one second is spent taking data, this one second arises because the scan rate and number of scans is identical, one second was chosen as a suitable timeframe for data to be averaged over so to minimise the effect of random

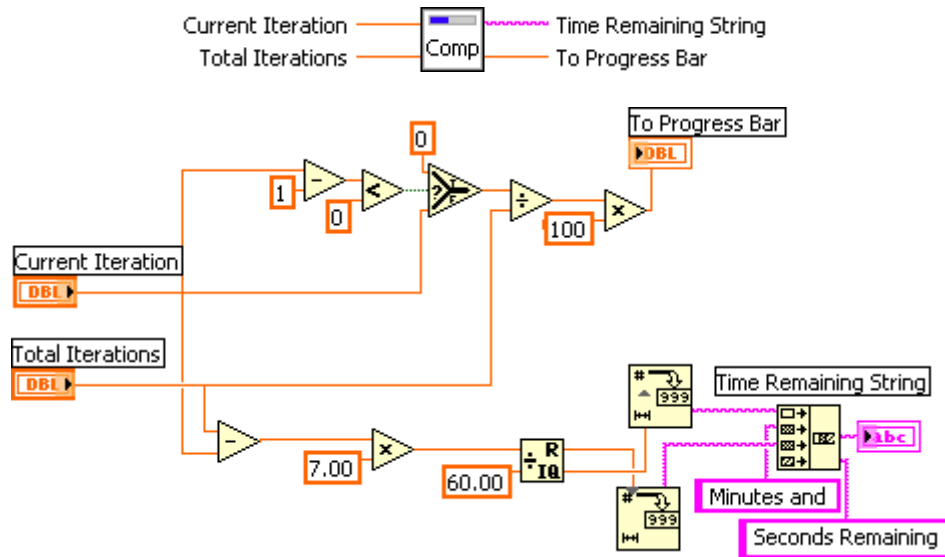
fluctuations in the system. Half a second is then given to the system to cease data collection activities before the next loop starts.

During the very first iteration of each run, an additional 10 seconds of waiting time is given to the system to allow the power amplifier more time to adjust. This extra time is given because when the power amplifier is turned on, it starts with zero output and takes much longer for it to reach its full output, than it would take to change its output by a small amount.

Progress Indicators:

The main Labview virtual instrument works by calling a selection of subvi's, then repeating the process again and again with slightly different input parameters. Without a progress indicator it is impossible to know how far through a run the program is and how long it should take to finish, to this end, a few loops of the program have been timed and this used to build up a progress bar and an indicator showing how much time is left.

Figure 23 - Labview progress indicator

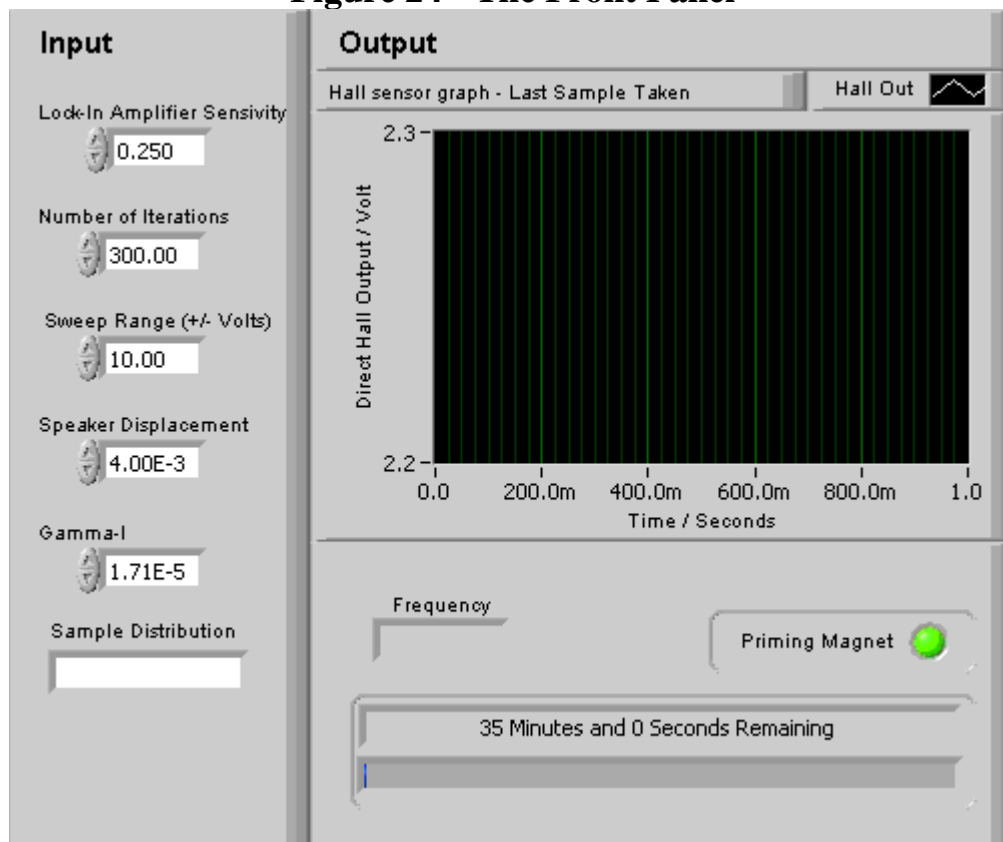


The two input parameters of this program are the current iteration and the total number of iterations, knowing how long one iteration takes leads directly to the time remaining.

The exact precision of this progress mechanism has not been tested, but it definitely gives a good impression of how much longer the user has to wait before the process is finished.

The Final Labview Virtual Instrument

Figure 24 - The Front Panel

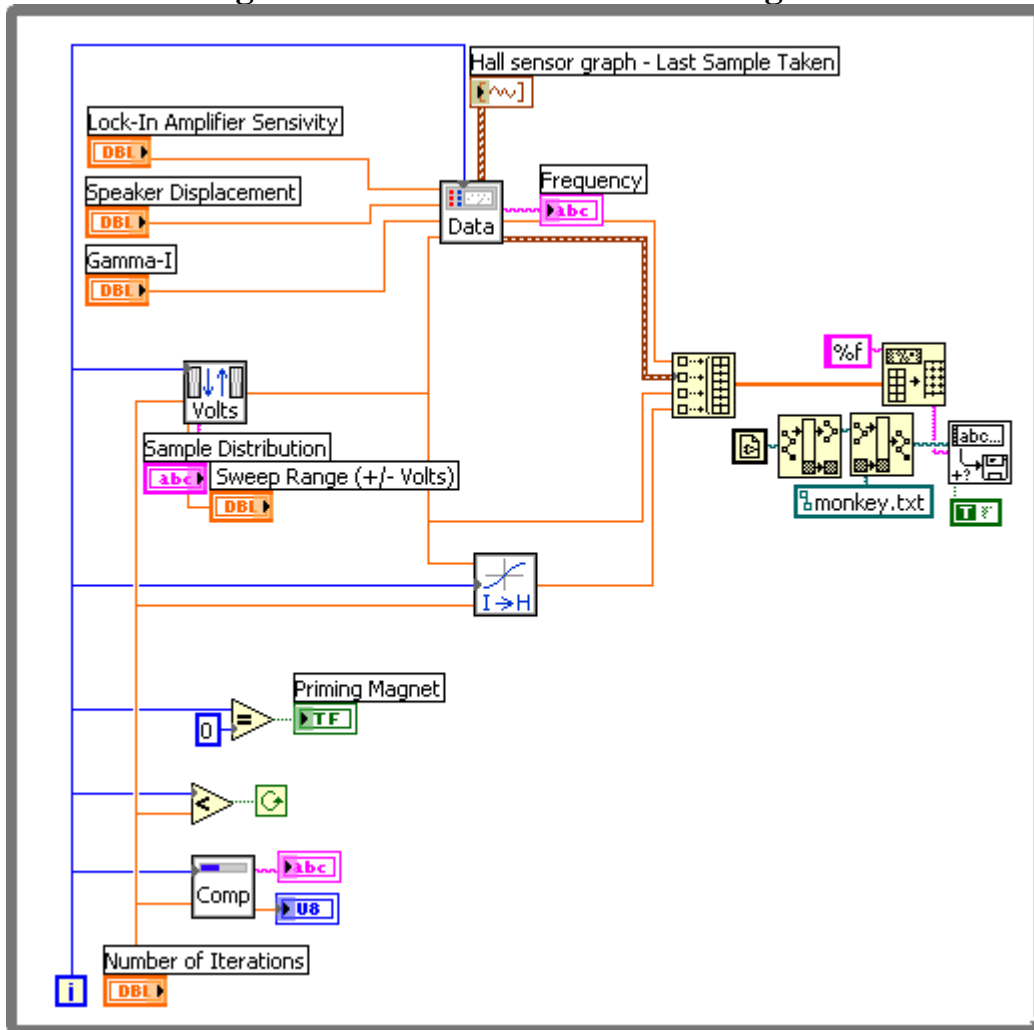


Figures 24 and 25 are the modularised interface and programming which are responsible for interfacing and calculations to generate magnetisation curves.

The program works by looping through iterations from 1 to I, where I is the total number of iterations, then stops. At the end of each iteration a selection of parameters are built together as an array and appended to a file “monkey.txt” in tab delimited form, the file resides in the same directory as the program is being run from. It is from this file which graphs can be plotted in excel and data manipulated, it would be possible to get Labview to read in all this data after the program terminates and get it to draw the graphs but it was decided that this would not add significant functionality to warrant the time being spent.

There is another level of interfacing below these virtual instruments, numerous virtual analogue channels have been set up which write and read differential voltages to and from various pieces of equipment. These are set up using the “Measurement and Automation Explorer” in the data network section with all references to them in the sub vi responsible for interfacing, figures 22, on figure 25 this is identified by the icon with the word “Data” on it.

Figure 25 - The Modular Block Diagram



Results:

Figure 26 - Magnetisation in Cobalt Wire - Orientation Data

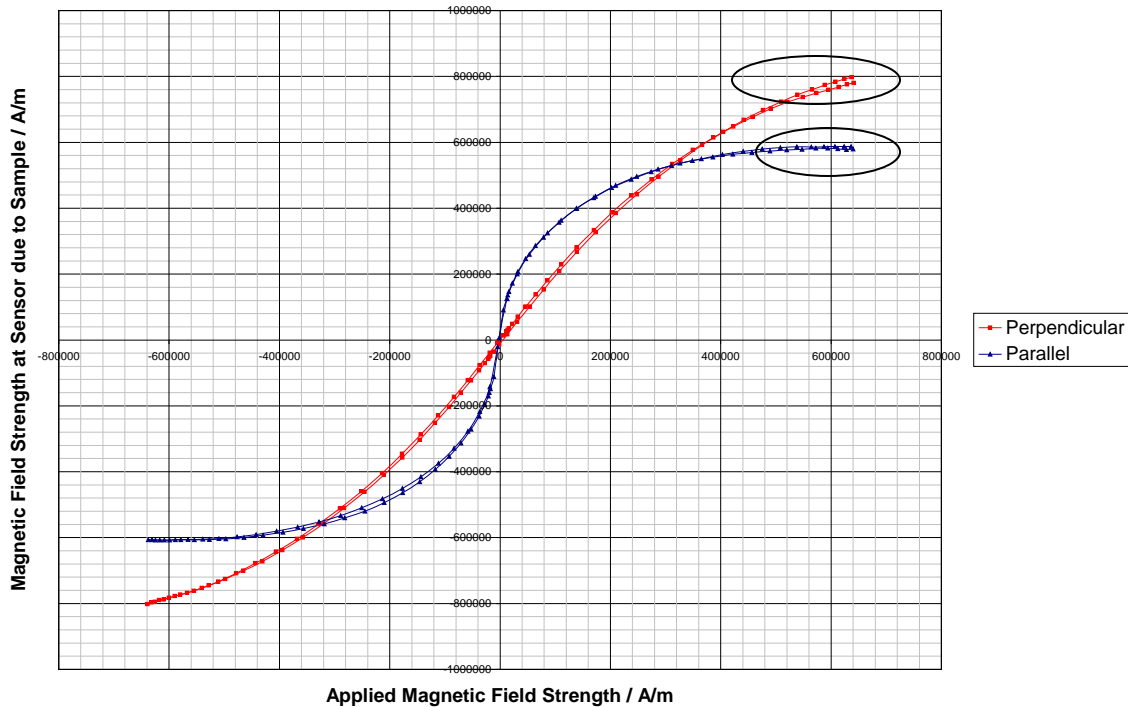
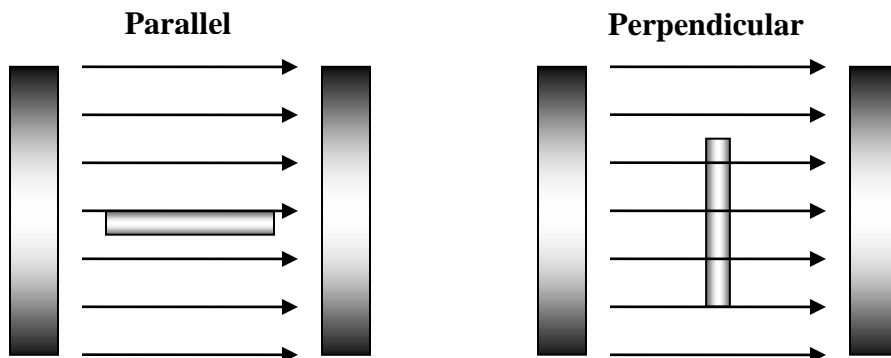


Figure 26 shows how the data collected from the system changes when the orientation of the sample relative to the field changes. The varying magnitude of magnetisation for the two curves are misleading, this is because the perpendicular sample presents a much larger surface to the hall sensor and the distance between the sample and hall sensor must be assumed to have changed, as a result in this case a higher detected magnetisation is observed. Corrections to this problem will be discussed at a later point.

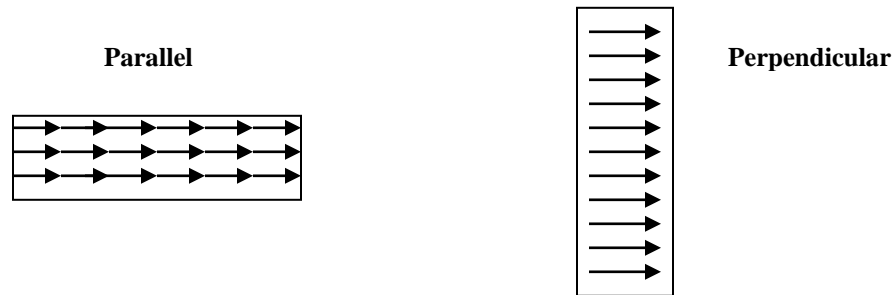
Figure 27 - Orientations of the cobalt wire in the field



The shape of the two curves implies that the sample magnetises easier when it is parallel to the field lines, than when it is perpendicular to them. This is likely to be because the parallel orientation is at a lower energy state where all the magnetic moments reinforce

each other, whereas when the sample is perpendicular there are numerous small parallel small moments in the sample. Figure 28 shows in an overly simplified way how the magnetic moments align inside the samples, the formation of one magnetic moment (indicated by an arrow) in the parallel sample will help to form another moment in the next domain, this effect is similar to van der Waals forces.

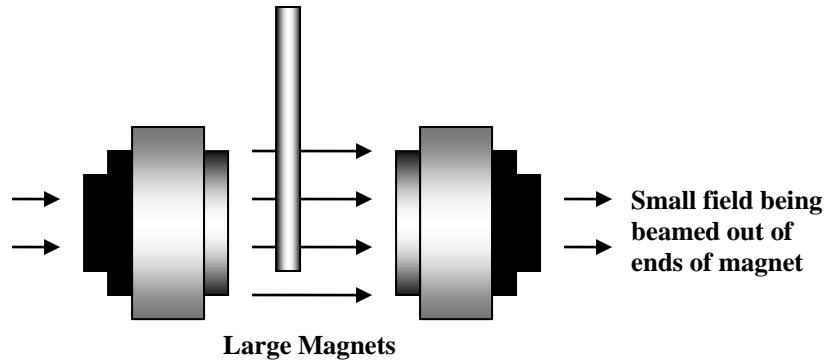
Figure 28 - Simplistic magnetic moment alignments



The manufacturing processes for making cobalt wire will inevitably involve it being drawn out into a wire shape, deforming the grain structures, this may have an effect on biasing the material to magnetise easier in one direction than the other. This will be investigated by measuring annealed cobalt wire in both orientations and comparing it to the plane cobalt wire, if the shapes of the differently orientated curves change relative to each other then this will indicate biasing by the drawing process.

An interesting issue in this graph is that at the positive magnetisation end, the loops appear to separate. It would be expected that the maximum magnetisation of the sample would be the same at the very start and end of the loop because the field surrounding it would be approximately the same. A causes for this drift has been established during the experimental work, the issue was when the frequency generator was physically on top of the lock-in amplifier and over time it causes the lock-in amplifier to lose phase, and subsequently not give the correct value for magnetisation, the cause of this is likely to be a result of magnetic fields inside the equipment interacting. When the equipment was spread out further the problem persisted but was less significant, to this end the large magnet was rotated by 90° in an attempt to stop it radiating out a large field in the direction of the equipment, this field was initially identified by the colours of a computer monitor being distorted; see figure 29.

Figure 29 - Beaming of the magnetic field



There is one other possible cause for this separation and it is that as the experiment runs, the power resistor which is used to measure current through the magnet rises in temperature. A rise in temperature will lower its resistance and hence the ratio of the resistance of the resistor to the magnetic coils, this will make the calibration for the field invalid. This heating effect also explains why the minus magnetisation ends join, the temperature and field at this end will be constant as the field changes direction. The only way to test this hypothesis would be to use a calibrated hall probe all the time and compare its field values over time to those produced by the calibration.

Consistency of the Magnetisation data

It is important to judge how reliable the readings of magnetisation are in comparison to each other, this repeatability is questionable because it is very hard to put a new sample into the VSM with exactly the same orientation relative to the hall sensor and field, most notable the distance between the sample and the hall sensor.

To this end, 5 pieces of cobalt wire were cut with all having approximately the same dimensions and each was inserted into the VSM parallel to the field and measured.

Cobalt wire dimensions:

Diameter = 1.000 ± 0.005 mm

Length = 14.24 ± 0.01 mm

Figure 30 - Repeatability of Magnetisation Value

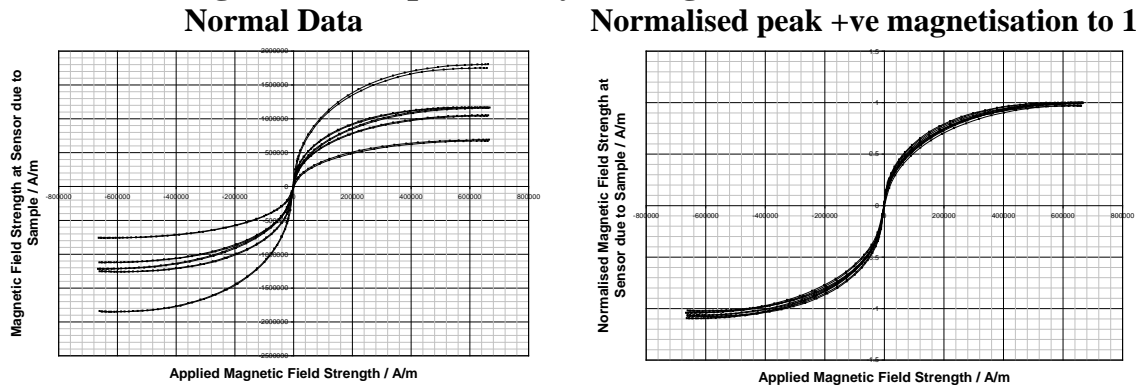


Figure 30 shows the magnetisation curves of 5 seemingly identical pieces of cobalt wire, the 'normal data' shows the significance of distance from hall sensor to sample resulting in a massive range of magnetisation values. It is clear that if magnitudes of magnetisation for different samples are to be compared then a more precise method of positioning the sample relative to the hall sensor is required. This would involve getting samples which exactly fit in the holes in the sample rod and the samples mean distance from the detector is constant or at least controllable and measurable.

The normalised data from the same figure shows that all 5 samples did not magnetise identically and there is some spread over the range of magnetisation shapes produced. The difference in shape of the loops is likely to be the result of the samples not being exactly parallel to the field. When each sample was placed into the sample rod, a normal distribution of angles of the sample relative to the field should be expected, from considerations of the magnetisation curves for the parallel and perpendicular samples, this seems reasonable.

Slight differences in the shape of the ends of the samples could also have some effect on the direction the field from the sample is beamed out. The end geometry looked similar to the eye but subtle differences could result in large differences in field at the hall sensor.

Investigating program timings

When the program is collecting data it allows a significant amount of time for all of the pieces of apparatus to adjust to a change before taking a reading, it is desired to see how the system would react if less time was given for the system to adjust before taking a reading.

Another way to simulate giving the system less time to adjust is to reduce the number of steps from which the magnetisation loop is to be made, this will increase the amount the system needs to adjust in between steps.

Figure 31 shows the current state of the system with timings shown in figure 22, the number of samples used to make up each loop has been varied from 50 to 10, with examples of 100 loops given previously in figure 26. The graph shows that as the step length is varies, the loop remains quite tight and there is no discernable trend produced when the number of samples is lowered, this shows that the timings which were previously decided on were very slack and gives the system more time than it need in-between readings.

Figure 31 - Affect of total iterations on magnetisation loops

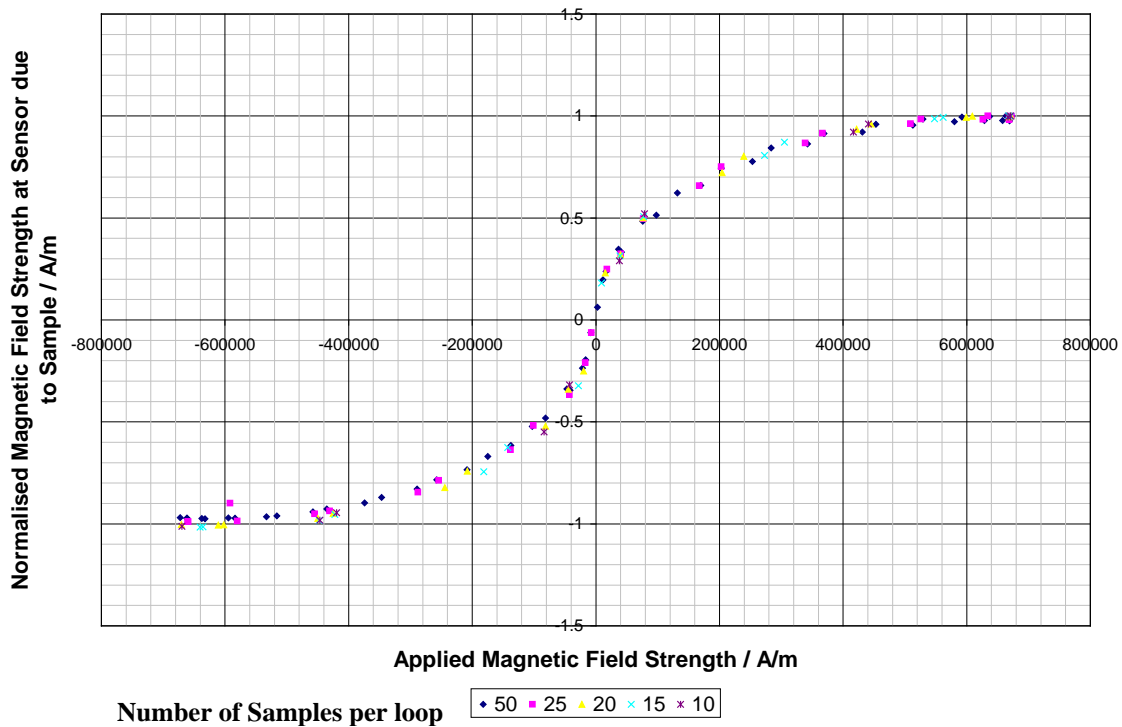
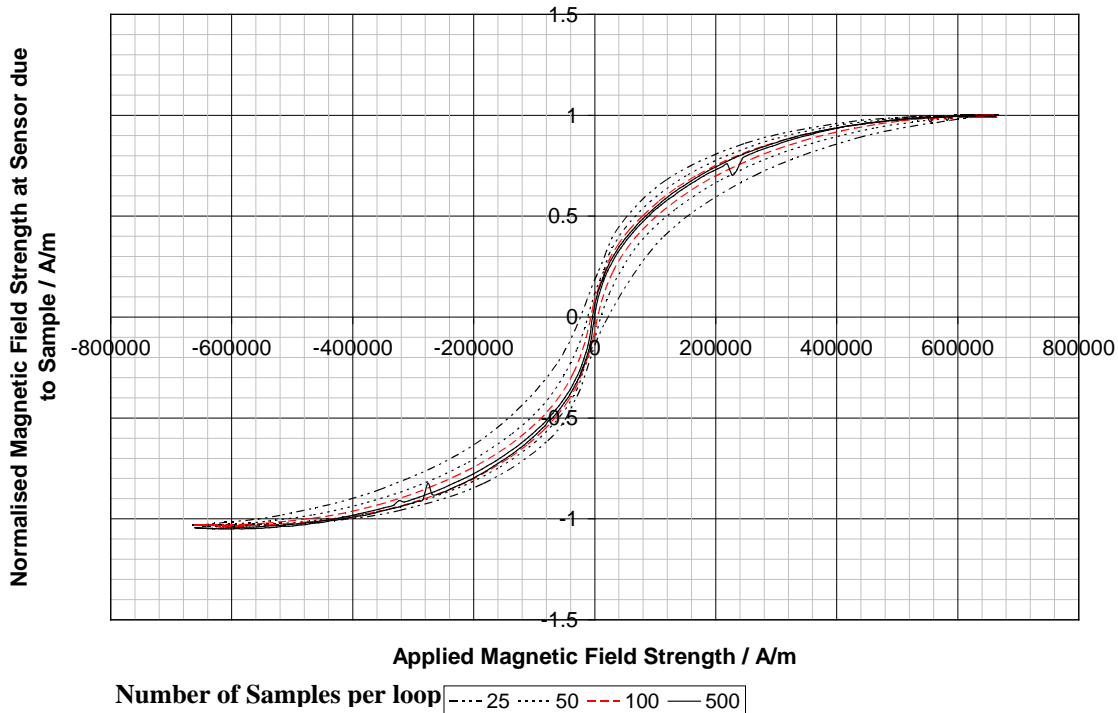


Figure 32 shows magnetisation loops produced by cutting out 4 seconds from the waiting time giving the system approximately 0.5 seconds wait between sets of readings. Reducing the waiting time has introduced a hysteresis loop which converges to a line as the number of samples is increased. From this it seems that as the rate of change of

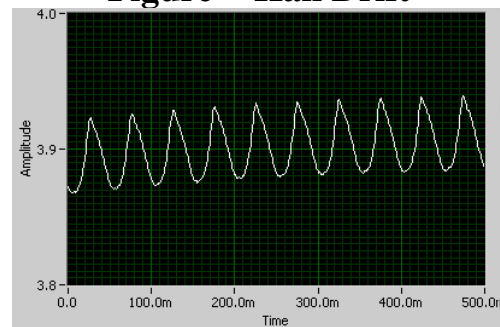
Labview output voltage passes a critical level the two sides of the loop start to visibly diverge.

Figure 32 - A reduction in the waiting time by 4 seconds



A sign that the system is not stable can be seen from examination of the output from the hall sensor. Under normal conditions the output from the hall sensor is an approximately sinusoidal wave but when the waiting time was reduced it was noticed that the wave tended to drift either up or down dependent on how far through the run the system was. This drift can be explained as the magnet not having fully adjusted its output, the field strength changes throughout the reading which is likely to confused the lock-in amplifier and give a false sense of the hall voltage.

Figure - Hall Drift



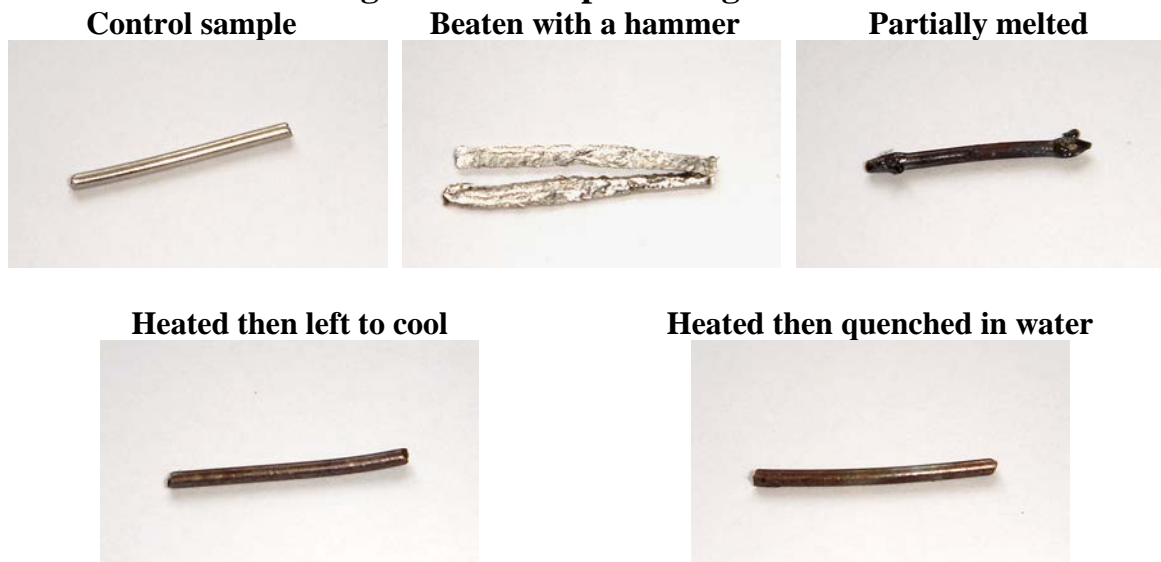
For these experiments the cosine distribution of voltages was used to drive the magnet, the fact that this distribution is centrally focused means that around the zero field level the rate of change of output voltage with time is smaller than expected. Examination of the outer loop with 25 samples implies that the effect of centrally focusing the distribution has clearly compressed the apparent hysteresis loop in the low field areas.

From this point onwards the cosine distribution will be used to collect data with 100 samples being used per loop, the waiting time for the loops will be the original values.

Altering Crystal Structures:

5 samples of cobalt were cut from the same piece of wire with approximately the same lengths, 4 out of 5 of them were then subjected to varying degrees of annealing in an attempt to alter their internal grain structures, and hence the way they magnetise.

Figure 33 - Samples being tested



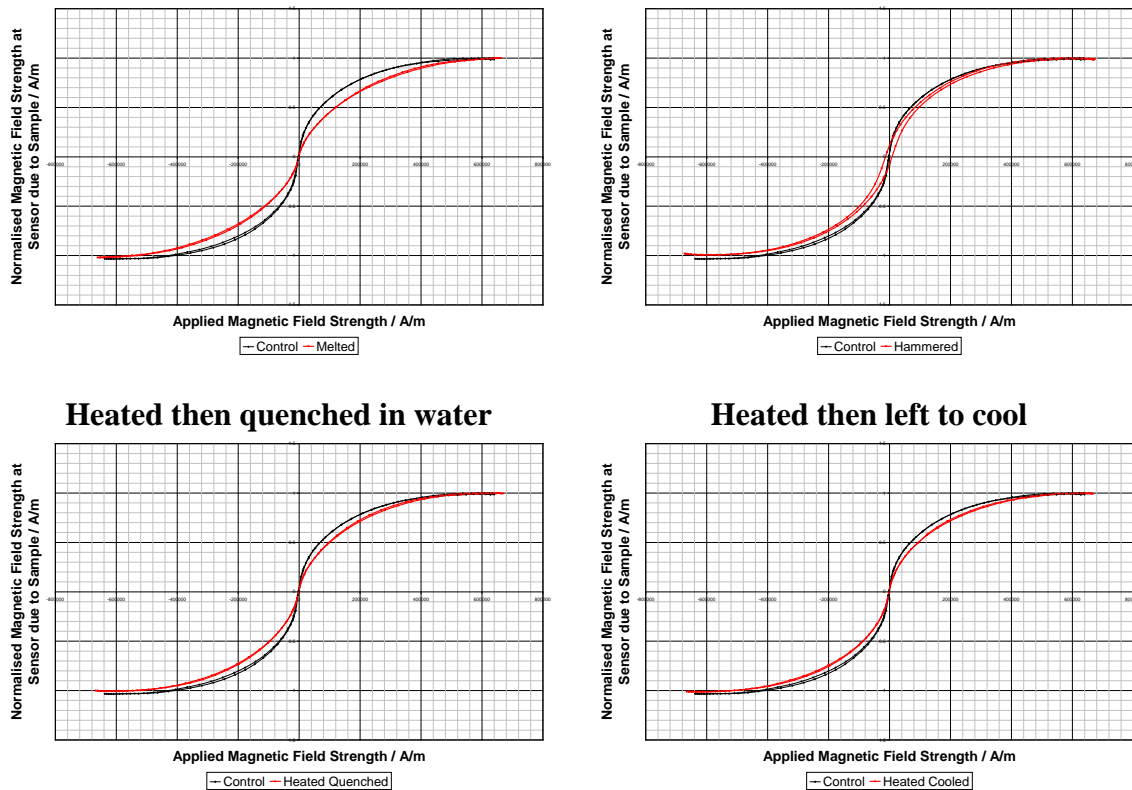
The sample which was partially melted was heated with an 'Oxy-Acetylene' welding torch and allowed to cool in air. The heating was stopped when the ends started to deform, this was to maintain a relatively constant shape to allow better comparison with other samples. Ideally the sample should have been full melted and recast into the same shape, but this was not possible. The other two heated samples were heated in a butane blow torch flame with a peak temperature of $\sim 1573\text{K}$, where the melting point of pure cobalt is 1768K .

Cobalt purity rated at 99.9%.

When the samples were annealed, they were done so in the magnetic field of the Earth and any other fields in the vicinity, this will introduce a permanent magnetisation into the samples but it is presumed that this is small and will have a negligible effect on the experiment. The cause of the permanent magnetisation is that during annealing the domain walls are free to move and will slightly align with the Earth's field, when annealing stops the domain walls freeze in a magnetised position.

The samples were placed individually into the VSM and the magnetism measured in both parallel and perpendicular orientations to the field. Figure 34 shows four plots with a parallel orientation, each one showing a comparison between the untouched cobalt wire and with different levels of annealing. As expected the process which produced the largest changes in magnetisation was the melting, this is because once the material starts to melt the grain structures are totally reformed which could have partially undone the distorted grain structure producing by the drawing process in production of the wire.

Figure 34 - Magnetisation curves of annealed Cobalt - Parallel Melted



The hammered sample which broke into two pieces shows an interesting change, it should first be noted that the two pieces were stuck together with tape to allow for conduction through the metal. Not only did the hammering affect the manner in which the sample magnetises as with the melting, it appears to have introduced a large hysteresis loop with the area inside the loop related to the energy lost per meter cubed of the cobalt. This hammering is likely to have introduced a lot of errors in the grain structure of the wire in comparison to a relatively error free drawn wire, all of these errors are likely to be the cause of the energy loss in the hysteresis loop as the domain boundaries get pinned into specific positions after magnetisation.

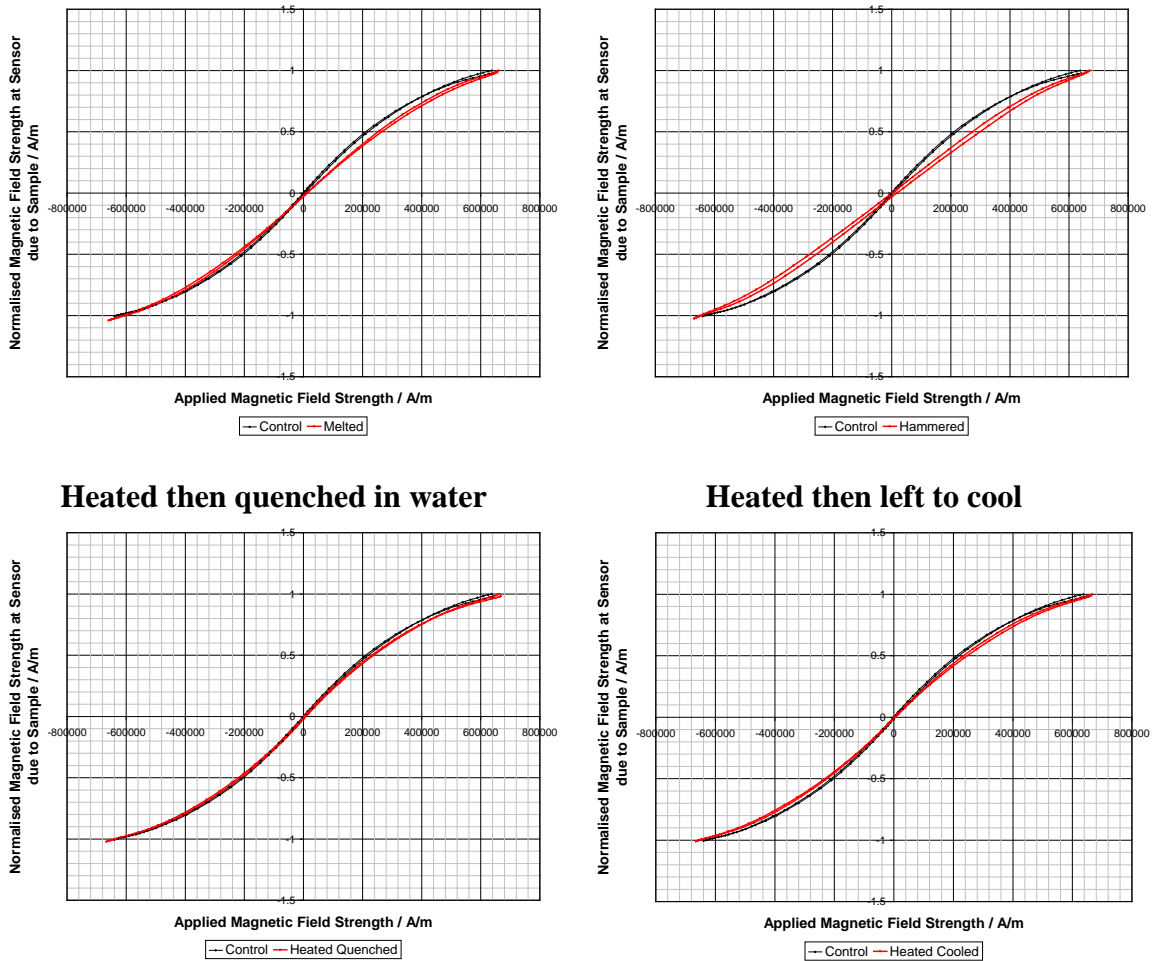
The two samples which were heated in the blow torch flame at a temperature less than the melting point have shown little change the manner in which they magnetise. From consideration of figure 30, it could be assumed that the difference in magnetisation from the control for both samples could be the result of random orientation errors; but the similarity between the two makes it more likely that the heating had a small effect but quenching one sample in water made no measurable difference.

Heating the samples with a blow torch could have slightly rearranged the grain structures in the material, it could have shifted around some of the errors in the crystal structure such as impurities, dislocations and such mentioned previously; this could have a slight effect on the manner by which the material magnetises. The reaction of the cobalt with

the air could have also oxidised part of the surface which may produce some interference with the formation of a magnetic field.

For completeness the data obtained from orienting the samples perpendicular to the field has been included. Figure 35 reiterates what was established previously from the parallel data with all the processes reducing the materials ability to magnetise in either orientation.

Figure 35 - Magnetisation curves of annealed Cobalt - Perpendicular
Melted **Hammered**



Permanent magnets

A small permanent magnet has been placed into the VSM and securely taped into place. Measurements were made to test if any hysteresis in the magnet was detectable and how the material having a permanent magnet moment would affect the magnetisation curves.

Figure 36 - Magnetisation curves from a permanent magnet

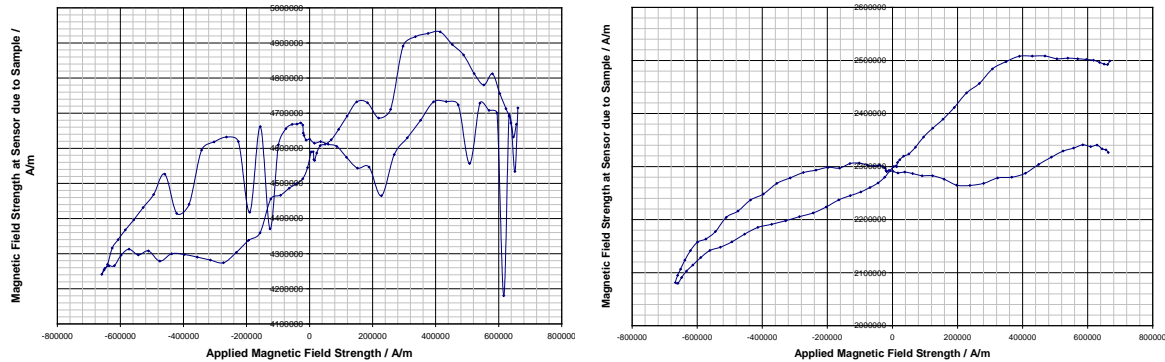
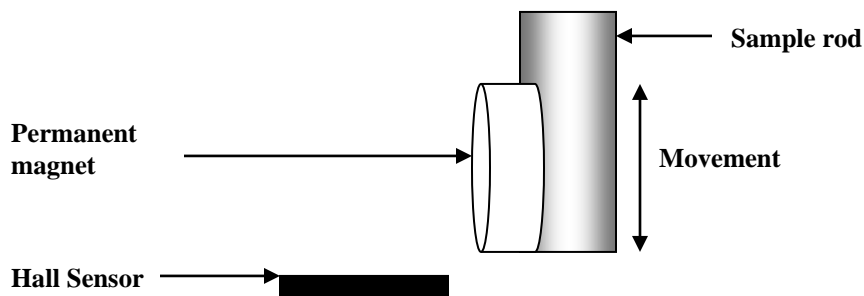


Figure 36 shows two graphs of magnetisation for the small permanent magnet, the left hand graph was obtained first, the large deviations from a smooth loop were theorised to be caused by movement of the magnet in the field, movement is hard to control because the small magnet is very strong and its interactions with a large field produce large forces.

The second graph was produced after re attaching the magnet to the sample rod, but this time it was mounted in blue-tack then taped heavily into place. This graph appears to show hysteresis in the negative field ranges and throughout the experiment a large drift in field strengths (ends in the top right quadrant do not match). If this graph is compared to the ideal hard ferromagnet (figure 2) then similarities seem to exist in the form of the area enclosed in the hysteresis loop, this is consistent with theory because permanent magnets exist as very hard ferromagnets so that they maintain a large magnetisation over time.

The point at which the magnetisation data crosses the y axis, the value should be proportional to the magnetism of the permanent magnet with the constant of proportionality being related to the distance between the hall sensor and the permanent magnet.

Figure 37 - Orientation of the Permanent Magnet

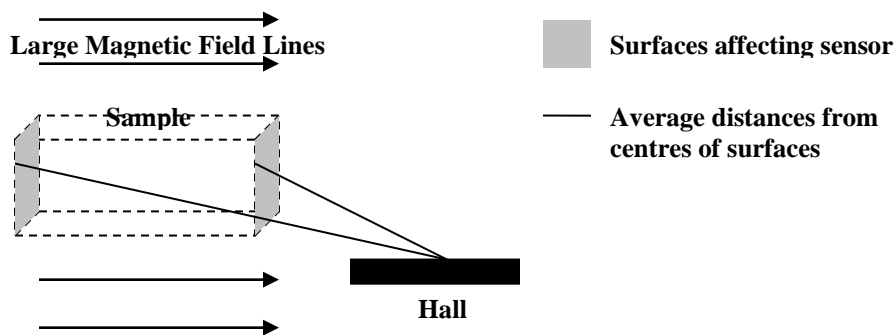


Conclusion:

This experiment did not reveal any quantitative magnetic properties of cobalt, the real problem was not being able to image the internal structures and how the magnetisation is changed with quantitative changes.

What was really needed was a conversion factor to change the magnetisation value to the true magnetisation of the sample. Finding such a factor would involve knowing the exact distances between the surfaces of the sample which could conceivably result in a field penetrating the hall sensor. For simple cases of a rectangular block (figure 38), finding the conversion factor would just involve two sides which both contribute but with cylindrical ferromagnets which have been annealed, there are many shaped surfaces which can contribute.

Figure 38 - Contributing fields at Sensor



Because the sample is oscillating up and down it will be necessary to use a RMS value of the distances. Before any of this could be calculated a better method of mounting the samples in consistent positions relative to the hall sensor would need to be established, and the wires would have to be perfectly straight and perfectly parallel to the field (perpendicular orientations would greatly complicate the calculations because of the curved shapes they present to the sensor).

Further investigation by measuring the electrical resistance of the pieces of cobalt wire may have led to some measurable relation, possibly the greater the resistance the larger the area enclosed in the hysteresis loop. This is consistent with the control sample and the sample which was hammered, the hammered sample clearly has a larger electrical resistance than the others because it has been beaten very thin.

Another very interesting experiment would be to measure how the magnetisation of a large single crystal of a ferromagnetic material varies with the angle it is to the direction of the field. In reference 6, there is discussion of which plane in the crystal structure produces the largest magnetisation.

References:

- [1] - <http://www.wordiq.com/definition/Crystal>
- [2] - Richard Feynman, Feynman Lectures on Physics, II 37-9
- [3] - Richard Feynman, Feynman Lectures on Physics, II 36-13 to 36-15
- [4] - Charles Kittel, *Introduction to Solid State Physics* (Wiley: New York, 1996). P449
- [5] - Flanders and Graham, Reports on Progress in Physics vol 56. P435-443
- [6] - Richard Feynman, Feynman Lectures on Physics, II 37-8

General References:

- Duffin, Electricity and Magnetism, 3rd Edition, Ch12 – P317+
(12.6 Ferromagnetic Materials: Hysteresis)
- <http://hyperphysics.phy-astr.gsu.edu/hbase/solids/hyst.html>
(Hysteresis)
- <http://hyperphysics.phy-astr.gsu.edu/hbase/solids/ferro.html#c4>
(Magnetic Domains)

Appendix:

Matlab code used to create cosine distribution mapping- figure 19

```
clear
x=linspace(0,2*pi,101);
y=abs(cos(x)); %creates 101 points for abs(cos(x)) between 0 and 2 pi
plot(x,y,'.') %plots cos(x) curve

hold on;
linear=[linspace(1,-1,51) linspace(-0.96,1,50)] %range from 1 to -1 to 1 with 101 points
plot(x,linear,'--') %plots the linear data points correctly positioned on cosine
plot(x,y.*linear,'b') %plots a multiplication graph
hold off;

%sets up axis
legend('y=abs(cos(x))','linear voltage +-1V','abs(cos(x))*linear voltage')
set(gca,'XTick',0:pi:2*pi)
set(gca,'XTickLabel',{'0','pi','2pi'})
xlabel('x')
ylabel('Voltage')
xlim([0 6.3])
```

Matlab code used to create squared distribution mapping- figure 20

```
clear
x=linspace(-1,1,101);
y=x.*x;
plot(x,y,'.') %plots cos(x) curve

hold on;
linear=linspace(1,-1,101) %range from 1 to -1 to 1 with 101 points
plot(x,linear,'--') %plots the linear data points correctly positioned on x*x
plot(x,y.*linear,'b') %plots a multiplication graph
hold off;

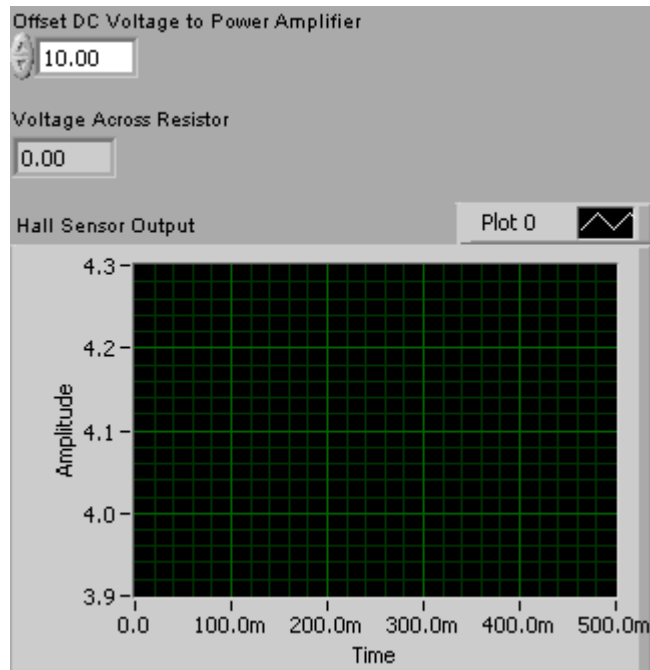
%sets up axis
legend('y=x*x','linear voltage +-1V','x*x*linear voltage')
set(gca,'XTick',-1:1:1)
set(gca,'XTickLabel',{'-total(i)/4','0','total(i)/4'})
xlabel('Iterations')
ylabel('Voltage')
xlim([-1 1])
```

The Calibration Program:

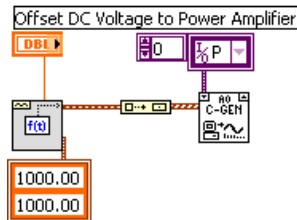
This is the experimental Labview VI which was used to check that the apparatus was working at the start of each session and after samples were changed.

This VI went under numerous rewrites throughout the project to allow it to be used to calibrate the apparatus instead of trying to do it with the main program. The beauty of this program is its simplicity, the DC offset voltage can be changed by using the keyboard and if the program is set to run continuously the hall sensor graph shows how long and what happens between transitions of field strengths. The program also outputs the voltage across the power resistor which is used to calibrate the field strength based upon the DC offset voltage. A non automated system for calibration is essential because it gives the user a greater appreciation of how the system works and ensures that for each reading, the system is stable.

Figure 39 – Calibration program



Driving signal for power amp



Hall Sensor Output Graph



Voltage from Power Amp Series Resistor

